Influence of Novel Zwitterionic Grafts on the Properties of Polypropylene, Ethylene-Propylene Rubber and their Blends

by

Andrew M. Powell

A thesis submitted to the Department of Chemical Engineering

in conformity with the requirements for

the degree of Master's of Applied Science

Queen's University

Kingston, Ontario, Canada

May 2015

Abstract

Polyampholyte derivatives of ethylene-propylene rubber (EPR-g-PA) and polypropylene (PP-g-PA) were prepared through the reaction a tertiary amino alcohol, 2- [2-(dimethylamino)ethoxy]ethanol (DMAEE), with maleated ethylene-propylene rubber (EPR-g-MAn) and maleated polypropylene (PP-g-MAn) respectively, forming zwitterionic grafts. The resulting zwitterionomers contained grafted ammonium and carboxylate functionality.

Conversion of EPR-g-MAn to EPR-g-PA substantially increased viscoelasticity and tensile modulus due to the presence of ionic associations between the polymer chains. EPR-g-PA showed similar viscoelastic properties to an EPR lightly cross-linked using dicumyl peroxide but with greater strain hardening and tensile elongation. Relative to its precursor material, EPR-g-MAn, EPR-g-PA exhibited equivalent adhesion to metals and improved adhesion to other ionomers, which was believed to relate to the presence of ionic associations at the substrate interface. The in-situ reaction of EPR-g-MAn with DMAEE during blending with PP produced a blend with superior impact properties compared to the thermoplastic vulcanizate (TPV) blend of peroxide cross-linked EPR and PP due to the elimination of peroxide induced degradation of the PP phase.

Conversion of PP-g-MAn to PP-g-PA had a negligible effect on its viscoelastic and mechanical properties. This was believed to relate to its low graft content, containing only 0.13 mol% grafted subunits. Despite its low graft content PP-g-PA was capable of forming strong associations with EPR-g-PA. Immiscible blends of EPR-g-PA and PP-g-PA exhibited improvements in droplet dispersion, tensile elongation and impact strength relative to their precursor blends of EPR-g-MAn and PP-g-MAn. Similarly, the addition of 7.5 wt% PP-g-PA to blends of 25/75 EPR-g-PA/PP was found to substantially improve droplet dispersion, impact strength and tensile elongation. These results suggest the preferential localization of PP-g-PA at the interface and the interaction of zwitterionic functionality across the phase interface, improving the compatibility between PP and EPR-g-PA. This conclusion was further supported

by the frequency dependent viscoelasticity of blends containing both PP-g-PA and EPR-g-PA which was found to deviate substantially from conventional immiscible blend behavior, exhibiting properties consistent with reactively compatibilized blends.

Co-Authorship

This thesis contains one chapter that presents results that have been published in the form of an original paper. The complete citation for this paper and the chapter in which it appears is provided below:

Chapter 3: A. Powell, M. Kontopoulou, S. Hojabr, *Macromol.React.Eng.* **2014**, *8*, 112-121.

This article was co-authored and reviewed prior to submission by Dr. M. Kontopoulou and Dr. S. Hojabr. All other work related to the current document has been prepared by the author with revisions by Dr. M. Kontopoulou.

Acknowledgements

I'd like to take this opportunity to acknowledge and thank some of those who supported me during the course of this degree.

To my supervisor, Dr. Marianna Kontopoulou I'm incredibly thankful for the encouragement, patience and guidance you've provided. Your positive attitude and counsel made this work possible and I can't sufficiently express my gratitude.

Financial support by Dupont/Queen's Innovation Programme (DuQuiP) and the Mitacs Accelerate program is gratefully acknowledged. Thanks to Dr. Sassan Hojabr, my supervisor at Dupont, for his assistance and insightful discussion during my stay there.

To my parents, Nicolle and James, your love and thoughtfulness made even the most difficult times manageable and I couldn't image these years without your support.

Table of Contents

List of Figures

List of Tables

List of Schemes

Nomenclature

Abbreviations

DCP	Dicumyl peroxide
DMA	Dynamic mechanical analysis
DMAEE	2- [2-(dimethylamino)ethoxy]ethanol
DSC	Differential scanning calorimetry
E/AA	Ethylene-acrylic acid copolymer
E/MAA	Ethylene-methacrylic acid copolymer
EHM	Eisenburg, Hird and Moore
EPDM	Ethylene-propylene-diene monomer
EPR	Ethylene-propylene rubber
EPR-g-MAn	Ethylene-propylene rubber with grafted maleic anhydride
EPR-g-PA	Ethylene-propylene rubber polyampholyte
EPR-Xlink	Cross-linked EPR-g-MAn
FT-IR	Fourier transform infrared
i-PP	Isotactic polypropylene
LDPE	Low density polyethylene
LVE	Linear viscoelastic
MAn	Maleic anhydride
MFI	Melt flow index
MFR	Melt flow rate
NBR	Nitrile-butadiene rubber
NR	Nitrile rubber
OC-Ionomers	Organic counterion neutralized ionomers

PA	Polyampholyte
PDI	Polydispersity index
PEVA	Polyethylene vinyl acetate
PP	Polypropylene
PP-g-MAn	Polypropylene-graft maleic anhydride
PP-g-PA	Polypropylene Polyampholyte
SAXS	Small angle X-ray scattering
SBR	Styrene-butadiene rubber
SEM	Scanning electron microscopy
SER	Sentmanat Extensional Rheometer
STEM	Scanning transmission electron microscopy
TEM	Transmission electron microscopy
TPE	Thermoplastic elastomer
TPO	Thermoplastic polyolefin
TPV	Thermoplastic vulcanizate

Symbols

G'	Storage modulus (Pa)
G"	Loss modulus (Pa)
G^*	Dynamic complex modulus of blend (Pa)
G^*_m	Dynamic complex modulus of matrix polymer (Pa)
G^*_d	Dynamic complex modulus of dispersed polymer (Pa)
η*	Complex viscosity (Pa.s)
ω	Angular frequency (rad/s)
δ	Phase angle

η_E^+ extensional stress growth coefficient (Pa.s)

$\dot{\varepsilon}$ Hencky strain rate (s^{-1})

d_n Number average droplet diameter (m)

d_v Volume average droplet diameter (m)

ΔH_m Heat of fusion (J/g)

T_g Glass transition temperature (^oC)

T_m Melting temperature (^oC)

T_c Crystallization temperature (^oC)

T_p Peak crystallization temperature (^oC)

T_i Onset crystallization temperature (^oC)

T_e Crystallization end temperature (^oC)

X_c Relative crystallinity

φ Phase volume fraction of blend

Γ° Equilibrium interfacial tension (N/m)

Chapter 1

Introduction

1.1 Background

Polypropylene (PP) is one of the largest commercial thermoplastics with global demand reaching 55 million tonnes in 2013 and accounting for approximately 25% of the total world polymer consumption.[1] Isotactic polypropylene (i-PP) is commonly used across a range of applications including packaging, automotive parts, containers, furniture and films for its heat resistance, ease of processability, rigidity, strength, low production cost and recyclability. Application of PP is however limited by its poor impact toughness.

Impact modification of PP is commonly achieved by blending it with ethylene-propylene rubber (EPR) forming thermoplastic polyolefin blends (TPO) with elastomeric EPR droplets dispersed within the PP matrix phase. Despite their similarity of structure ethylene-propylene rubbers are generally incompatible with isotactic polypropylene, forming immiscible blends.[2,3] The properties of these blends are consequently limited by their poor morphological stability, large domain sizes and low interfacial adhesion. To further improve the properties of these blends several strategies are commonly employed including: crosslinking of the elastomer phase forming thermoplastic vulcanizates (TPVs), addition of an interfacial compatibilizer and manipulation of processing conditions.

Ionomers are polymers containing small amounts of grafted ionic functionality that have attracted substantial attention for their highly polar functional groups capable of forming strong ion-ion and ion-dipole interactions.[4] The ion-ion interactions between ionomer chains behave like thermoreversible crosslinks, forming physical cross-links at service temperature while maintaining melt processability at elevated temperatures.[5] Ionomers are consequently of interest as alternatives to conventional thermoplastic elastomers. Commercial ionomers are typically prepared through neutralization of carboxylic and sulfonic acid groups with metal counterions. Even though the use of organic counterions

offers a greater range of cation structure and further means of tailoring ionomer properties, they typically form weaker associations, exhibiting only marginal increases in viscosity and elasticity following neutralization.[6,7]

Ionomers have also been shown to act as effective interfacial modifiers, improving blend compatibility by forming strong interactions at the phase interface.[8] The addition of metal neutralized ethylene-methacrylic acid ionomers to PP and ethylene propylene diene monomer rubber (EPDM) has been shown to enhance phase miscibility, improving droplet dispersion and material toughness.[9,10]

Given the predominance of PP in industry a means of effectively improving its impact resistance is of some commercial importance. The toughening of PP with an ionomeric thermoplastic elastomer could offer several potential advantages over conventional thermoplastic elastomers, including the capacity to form thermoreversible ionic physical crosslinks and the potential to form strong associations across the blend interface with other functionalized polymers.

Lee et al.[11] synthesized an ionomer from the reaction of maleated polyethylene with a tertiary amino alcohol, exhibiting large increases in viscoelasticity atypical of most ionomers synthesized using organic counterions.

This method of introducing strong ionic associations based on organic counterions into maleated polymers may offer a means of synthesizing novel ionomer thermoplastic elastomers and ionomeric compatibilizers which may contribute to the toughening of thermoplastic polyolefin blends of PP and EPR.

1.2 Objectives and Outline

Given potential value of ionic associations in TPO blends the main objectives of this work were:

1. To synthesize and investigate the properties of novel polyolefin-based ionomers generated by the reaction of maleated PP and maleated EPR with a tertiary amino alcohol.

2. To investigate TPO blends of PP and zwitterionic EPR and to examine their potential application as alternatives to conventional thermoplastic vulcanizates cross-linked using peroxides.
3. To investigate the efficacy of a PP zwitterionomer as a compatibilizer for blends in PP/EPR zwitterionomer blends.

This dissertation is divided into five chapters. Chapter 2 reviews the literature of ionomers with an emphasis on the application of ionomers in thermoplastics. Chapter 3 investigates the properties of an EPR ionomer and its blends with PP through a detailed examination of blend morphology, rheology and mechanical properties as potential alternatives to TPVs. Chapter 4 investigates the properties of a PP ionomer and its effectiveness as a phase compatibilizer in blends of PP and ionomeric EPR through its effect on morphology, mechanical properties and viscoelastic behavior. The thesis finishes with Chapter 5 which summarizes the main conclusions of the work and provides recommendations for future work.

1.3 Work Cited

[1] Ceresana, *Market Study: Polypropylene*, 3rd edition 2014.

[2] L. D'orazio, C. Mancarella, E. Martuscelli, F. Polato, *Polymer.* **1991**, *32*, 1186-1194.

[3] L. D'orazio, C. Mancarella, E. Martuscelli, G. Sticotti, P. Massari, *Polymer.* **1993**, *34*, 3671-3681.

[4] A. Eisenberg, J. Kim, *Introduction to Ionomers*, Wiley, New York 1998.

[5] D. J. Yarusso, S. L. Cooper, *Polymer.* **1985**, *26*, 371-378.

[6] H. Xie, D. Liu, D. Xie, *J Appl Polym Sci.* **2005**, *96*, 1398-1404.

[7] R. A. Weiss, P. K. Agarwal, R. D. Lundberg, *J Appl Polym Sci.* **1984**, *29*, 2719-2734.

[8] P. Smith, A. Eisenberg, *J.Polym.Sci.B Polym.Lett.Ed.* **1983**, *21*, 223-230.

[9] Y. Kim, C. Ha, T. Kang, Y. Kim, W. Cho, *J Appl Polym Sci.* **1994**, *51*, 1453-1461.

[10] Y. Kim, W. Cho, C. Ha, W. Kim, *Polym.Eng.Sci.* **1995**, *35*, 1592-1599.

[11] J. A. Lee, M. Kontopoulou, J. S. Parent, *Polymer*. **2005**, *46*, 5040-5049.

Chapter 2

Literature Review

This thesis investigates the effects of novel zwitterionic functionality on polymer and blend properties and this section examines concepts that are important in understanding and justifying its work. The fundamental properties of ionomers are explored, with a particular emphasis on ionomer thermoplastics containing functionality similar to the ionomer under investigation.

2.1 Ionomers

2.1.1 History

In the mid 1960's DuPont introduced the first commercial ionomer, an ethylene-methacrylic acid based ionomer under the trade name Surlyn®, synthesized by the addition of sodium hydroxide or zinc hydroxide to a random copolymer of ethylene and methacrylic acid.[1,2] The neutralization of the carboxylic acid groups with metal cations generated metal cation/carboxylate complexes, see Scheme 2.1. These ionic functional groups were found to form strong electrostatic interactions with each other between chains generating a polymer with high melt viscosity and superior tensile properties.

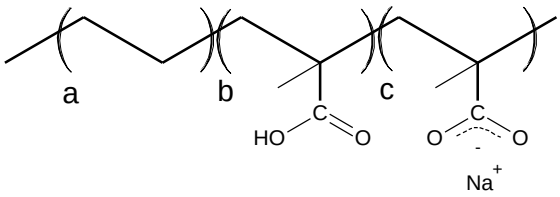

Scheme 2.1. Typical chemical structure of ethylene methacrylate ionomer partially neutralized with NaOH with monomers in brackets: a) ethylene, b) methacrylic acid, c) methacrylic acid neutralized with sodium.

2.1.2 Ionomer definition

The term ionomers has since been used to describe polymers that contain small amount of ionic functionality, up to 15 mol%, bound as pendant groups to the hydrocarbon chains.[3] Though polymers with higher ionic concentration are typically referred to as polyelectrolytes the ionic concentration over which a polymer is considered an ionomer varies heavily depending on the functionality of the polymer and may display properties of either or both ionomers and polyelectrolytes.[4] While the content based classification is still commonly used, an alternative definition was proposed by Eisenberg et al. to reduce the ambiguity in the classification of ionomers and polyelectrolytes:

Ionomers are "polymers in which the bulk properties are governed by ionic interactions in discrete regions of the material" and polyelectrolytes are "polymers in which solution properties in solvents of high dielectric constants are governed by electrostatic interactions over distances greater than typical molecular dimensions".[5] "Discrete regions" refers to the formation of areas of high ionic concentration within the bulk which may restrict motion of the contributing polymer chains.

2.1.3 Ionomer morphology

Within ionomers ion-pairs are present in a low dielectric medium and consequently they attract one-another by electrostatic forces to generate groups of ion-pairs. These areas of high ionic concentration are

described by the multiplet-cluster model.[6] A multiplet, illustrated in Figure 2.1, defines a group of directly interacting ion-pairs, typically 2-8 pairs. Clusters describe ion-rich areas that are comprised of several multiplets.

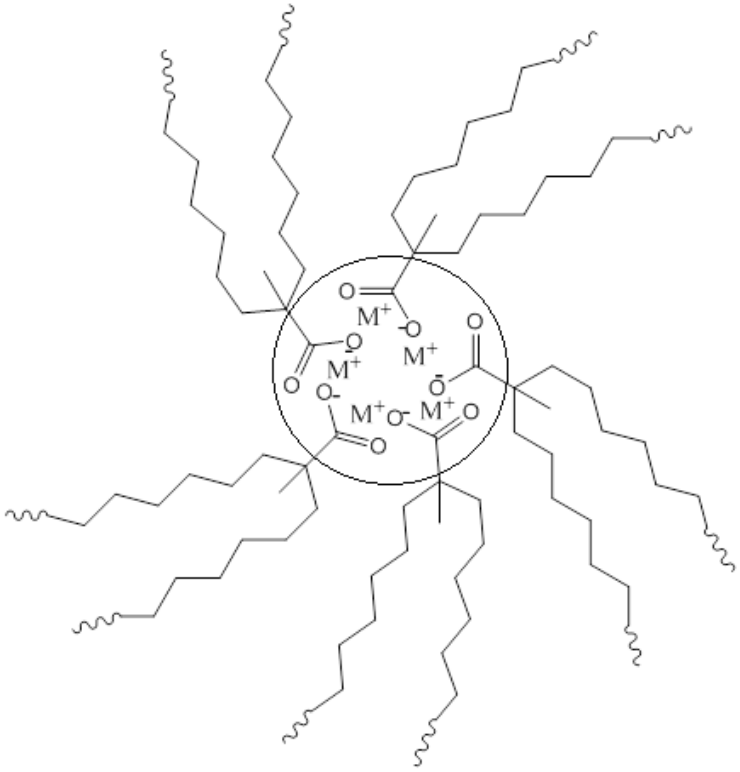

Figure 2.1. Depiction of multiplet structure containing metal-carboxylate ion-pairs.

This multiplet-cluster model was further refined by Eisenburg, Hird and Moore, known as the EHM model, to explain ionomer viscoelastic behavior. This model describes the morphology surrounding ionomer multiplets as the "restricted mobility layer", a region of reduced polymer chain mobility compared to the bulk properties. [7] This model further defines clusters as an aggregation of ion-pairs with a region of restricted mobility sufficiently large to exhibit their own glass transition temperature.

A wide range of techniques have been used to examine the presence and structure of clusters in ion containing polymers, the most influential of which are: small angle X-ray scattering (SAXS) and scanning transmission electron microscopy (STEM). Morphological studies using these techniques have found that

clustering is heavily determined by ionic concentration, typically only forming beyond a threshold concentration (2-6 mol% ionic subunits), with sizes ranging between 2-10 nm in diameter.[6,8,9]

2.1.4 Properties of thermoplastic ionomers

The introduction of ion-pair domains, both multiplets and clusters, into a polymer generates physical cross-links between polymer chains, the extent of which are governed by the strength of electrostatic force between ion-pairs and ionic concentration. These physical cross-links behave much like covalent cross-links and can influence viscoelastic properties, increasing modulus and extending the temperature range of rubbery behavior.[3,10]

The most common class of ionomers are those based on poly (ethylene-co-methacrylic acid) (E/MAA) and poly (ethylene-co-acrylic acid) (E/AA). These acid-copolymers are typically neutralized with metal cations (e.g. Na^{+}, K^{+}, Zn^{2+}, Mg^{2+}) to generate ionomers with ionic content between 2-10 mol%. In addition to a large increase in tensile modulus and viscosity, the introduction of ionic functionality into these polymers can substantial alter their thermal behavior, increasing the onset temperature of crystallization due to nucleation at the zwitterionic sites while slowing the rate of crystallization due to their lower chain mobility.[11]

2.2 Ionomer Thermoplastic Elastomers

Thermoplastic elastomers (TPEs) have emerged in the last 50 years as alternatives to vulcanized rubbers, displaying elastomeric properties while maintaining the melt processability of a thermoplastic.[10] Their thermoplasticity confers a number of advantages over conventional rubbers:

- High degree of control over properties through multi-component blending
- Flexibility in processing; they can be processed through range of methods unsuitable for thermosets: thermoforming, blow-molding, injection molding, etc.
- Reduced processing requirements, including shorter cycles and reduced energy cost.
- Material easily recycled and reprocessed, reduced waste.

TPEs are capable of having a network of strongly linked polymer chains while maintaining their thermoplasticity through the use of reversible physical cross-links rather than the covalent cross-links of cured elastomers. These physical cross-links are generally based on phase separated systems in which one phase behaves as a solid effectively linking the chains of the other amorphous phase. This can be achieved through a wide range of structures including: block copolymers, thermoplastic polyolefin (TPO) blends, and ionomeric thermoplastic elastomers.[10,12]

Ionomeric TPEs contain ionic functionality bound to their hydrocarbon chains and derive their elastomeric properties from the physical cross-links between these charged groups. TPEs based on this ionic functionality are of commercial value because of their capacity to exhibit the mechanical properties of vulcanized rubber while maintaining their thermoplasticity.

Conventional ionomer thermoplastic elastomers are based on neutralization of carboxylated or sulfonated ethylene-propylene-diene monomer (EPDM) systems. While these elastomers can exhibit mechanical properties similar to their covalently cross-linked polymers their melt state behavior is fundamentally different.[13] Covalent cross-linking forms irreversible networks between the polymer chains limiting or preventing flow at higher cross-link densities. Ionomers, however, are able to melt even with very high ionic concentrations. While this behavior suggests the dissociation or partial dissociation of ion-pair clusters and multiplets at higher temperature it hasbeen found that these domains tend to persist even beyond polymer degradation temperatures.[14,15] Ionomer flow is believed to occur in the presence of ion-pair associations through the mechanism of "ion-hopping" whereby ion-pairs may move between adjacent ionic-domains by micro-Brownian motion of short chain segments.[16-18]

2.3 **Ionomers with organic counterions (OC-Ionomers)**

Ionomer morphology and properties are strongly influenced by the type of counterion used to neutralize the acid-functional groups. The effect of inorganic counterion on ionomer properties has been well studied and recent morphological studies have linked changes in metal cation type to changes in the size of ionic clusters and their structure.[19-21] Changing the size and type of the cation can influence the

cation-anion distance and interaction energy between ion-pairs and consequently influence the thermal, mechanical, rheological and conductive properties of the ionomer.[7,13,22] .

While it is understood that the selection of the appropriate counterion is important in controlling ionomer properties, a manufacturer's degree of control is constrained by the finite selection of inorganic counterions and their structural similarities. Organic counterions as an alternative to metal based cations are consequently of interest due the wide range of organic structures available and for the ability to tailor these structures to obtain the desired ionomer characteristics.

Organic counterions have become a focus in polyelectrolytes due their high mobility and recent research has focused heavily on their potential as biocides and filtration membranes,[23-25] however they have shown little value as thermoplastic elastomers compared to conventional ionomers.

A wide range of polymers and organic ionic complexes have been reported.[26-32] The majority of these polymers are prepared by neutralizing pendant sulfonyl or carboxyl groups with alkylamine and alkylphosphine derivatives. Common organic counterions are shown in Scheme 2.2.

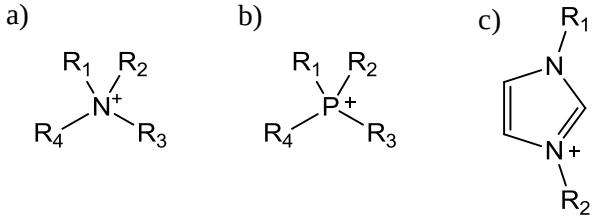

Scheme 2.2. Conventional organic counterions derived from: a)ammonium, b)phosphonium or c)imidazolium. R-groups typically: H, alkyl or alkyl ether chains with 1-4C

Consistent with metal-ionomers, ionomers neutralized with organic counterions (OC-ionomers) are capable of forming multiplets and clusters, however due to the size of their ion-pairs these clusters are typically much larger.[33,34] Though morphologically similar, OC-ionomers typically have much weaker

associations than their analogous metal-ionomers and consequently show much smaller changes in rheological, mechanical and thermal properties.[26,30]

The viscoelastic properties of OC-ionomers are heavily influenced by the structure of the organic counterion. Increasing alkyl group substitution and substituent size can limit physical cross-linking between ion-pairs through steric hindrance and electron shielding, reducing the glass transition temperature (Tg), viscosity, modulus and tensile strength.[26,31,35] .

Weiss et al.[26] investigated the effect of ammonium structure on the rheological and thermal properties of sulfonated polystyrene ionomers and compared these results to those of their precursor materials across a range of functional group concentrations (1-20mol%). The majority of the ammonium based ionomers tested were found to have similar Tgs and equivalent or lower viscosities compared to the un-neutralized sulfonated polystyrene. Primary amines increased viscosity while tertiary amines had marginal or negative effect. An analysis of the dynamic mechanical properties of sulfonated (2.3mol%) polystyrene ionomers showed similar trends:[36] neutralization with metal ions (Na^+,K^+,Rb^+,Cs^+) generated materials with higher moduli and longer rubbery plateaus, neutralization with trimethyl ammonium counterions had a negligible effect on the moduli and larger ammonium counterions (tripropyl ammonium and tributyl ammonium) greatly reduced the breadth of rubbery plateau.

Though versatile in structure, organic counterions are of limited value in the formation of ionomeric thermoplastic elastomers. Neutralizations with small organic counterions can improve viscoelastic properties, however these changes are typically less than conventional metal counterions and their volatility can limit their means of preparation. Though OC-ionomers with larger alkylammonium and phosphonium counterions can easily be synthesized though reactive compounding they typically have lower viscoelastic properties compared to their precursor materials due to their diminished functional group association.

2.4 Zwitterionomers

Zwitterionic functional groups are electrically neutral molecules, or polymer branches, that bear both positive and negative formally charged substituent groups, separated by electrically neutral non-conjugating intervening atoms, see Scheme 2.3. Zwitterionic functional groups in polymers are of interest because of their ability to form strong intermolecular associations in matrices of low dielectric constant.[37,38] Though zwitterion groups in polyzwitterions have been studied extensively for their aqueous application and their anti-fouling properties,[39,40] little attention has been given to zwitterion based ionomer thermoplastics. This section reviews zwitterionic thermoplastic elastomers in literature, with a focus on the effect of zwitterionic functionality on their mechanical and viscoelastic properties.

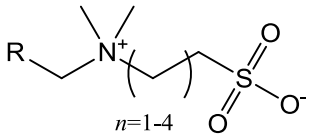

Scheme 2.3. Typical zwitterionic functionality with sulfobetaine structure in zwitterionic polymers.

2.4.1 Zwitterionomer structures

Nomenclature of zwitterion containing polymers has been inconsistent and depending on their structure may be referred to as one or more of the following: zwitterionomers, polyzwitterions, polyampholytes, polybetaines. Though these terms are frequently used interchangeably ionomer thermoplastics containing zwitterionic functionality are conventionally referred to as zwitterionomers.

The majority of zwitterionomers in literature are based on copolymers incorporating a sulfo-ammonium zwitterionic group as shown in Scheme 2.3. These zwitterionomers are structurally similar to conventional ionomers forming multiplets and clusters with increasing ionic concentration. Morphological analyses of n-butyl acrylate sulfobetaine zwitterionomers by SAXS and DSC suggested that zwitterionomer clusters are consistent with predictions by the EHM model, with regions of restricted mobility surrounding ionic domains.[41,42] Clusters of ammonium-sulfonate zwitterionic groups in poly (4-

vinyl pyridine-sulfopropyl betaines) (4 mol%) have been viewed by TEM with domain sizes (5-20 nm).[43] .

2.4.2 Properties of zwitterionomers

Though zwitterionomer morphologies have some structural similarity to alkyl-ammonium neutralized ionomers, their viscoelastic properties are more consistent with metal neutralized ionomers, where the incorporation of zwitterionic functionality results in large increases in viscoelastic properties.

Work by Galin et al. examined n-butyl acrylates containing sulfopropyl ammonium zwitterionic groups, and compared their solid-state properties to n-butyl acrylates of similar respective molecular weights.[42,44] Dynamic mechanical analysis (DMA) showed a large increase in modulus and the development of a rubbery plateau with increasing ionic concentration . The formation of a second high temperature Tg and the presence of an ionic peak by SAXS at ion concentrations beyond 4mol%, suggested a large degree of phase separation similar to metal neutralized ionomers.

Polyurethane zwitterionomers have shown similar results with introduction of sulfopropyl ammonium zwitterionic groups.[45] DMA across a wide range of polyurethanes showed an increase in modulus and length of the rubbery plateau with concentration of zwitterionic functionality. Incorporation of these groups also had a dramatic effect on tensile properties showing an increase in Young's modulus by a factor of 2 with incorporation of 3 mol% zwitterionic groups.[46]

The effect of the quaternary ammonium structure was examined across a wide range n-butylacrylate and ethoxylethylacrylate sulfobetaine zwitterionomers.[47] DMA of these copolymers showed a decrease in modulus and rubbery plateau with increasing bulkiness of quaternary ammonium group due steric hindrance of ion-pair interactions. The effect of ammonium cation size on zwitterionomer properties is similar to its effect on alkylammonium neutralized ionomers, though the zwitterionomers consistently showed greater viscoelastic properties than their alkylammonium neutralized analogues.

The strength of the associations between zwitterionic groups and the resulting viscoelastic properties of zwitterionomers have been largely attributed to the large dipole moments of zwitterionic structures with

short intercharge separation, with typically less than 6 carbons between charged groups, see Scheme 2.3 (n<5) and the direct association of the anions and cations covalently bound to two separate polymer chains. [37,38,48] This direct inter-chain ion-pairing is distinct from conventionally neutralized ionomers which are based on the formation of multiplets of associating ion pairs, see Figure 2.2.

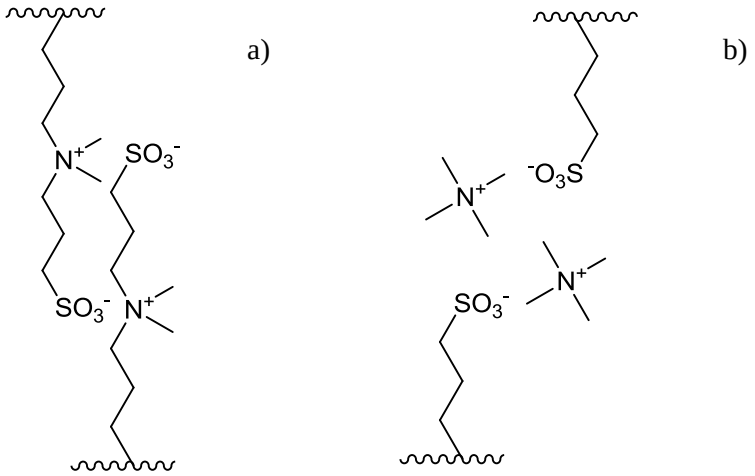

Figure 2.2. Illustration comparing ion-pairing structure of zwitterionomers to conventional ammonium-sulfonate ionomers.

This difference in ion-pairing may in part explain the differences in properties between OC-ionomers and zwitterionomers. A study comparing n-butylacrylate copolymer with ammoniopropanesulfonate zwitterionic groups to an analogous ionomer with quaternary ammonium groups neutralized by sulfonate groups observed greater phase separation and elasticity in the zwitterionomer. The zwitterionomer displayed a rubber plateau at relatively low ionic content (6mol%),which was not present in the conventional ionomer even at high ionic content (15mol%).[48]

These studies suggest that zwitterionic functionality in polymers may provide stronger associations than ionomers neutralized by organic cations while offering the flexibility of design inherent to organic compounds. Despite evidence of their strong associations and potential value as a versatile alternative to

conventional ionomer thermoplastic elastomers the zwitterionomers in literature are predominantly based on variations of the same functionalities: carboxy and sulfo-betaines.[3,10,39]

2.4.3 Succinic anhydride derived zwitterionomers

A novel zwitterionic functionality was reported during the reaction of maleated (3.4 wt%) ethylene-propylene random copoloymer (EPR-g-MAn) with N,N-dimethylethylenediamine.[49] At higher temperatures this reaction generated a cyclic imide, however at room temperature it yielded a thermally unstable zwitterionic intermediate. Gelation of the reaction mixture suggested the formation of a physically cross-linked network, however its irreversible conversion to the imide at higher temperatures made this zwitterionomer unsuitable for conventional polymer processing.

Recent work by Lee et al. prepared and examined the properties of a similar zwitterion-containing polymer produced by the reaction of a tertiary amino alcohol, dimethylaminoethoxy ethanol (DMAEE), with the succinic anhydride groups of maleated polyethylene (PE-g-MAn, 1wt% pendant succinic anhydride), see Scheme 2.4.[50]

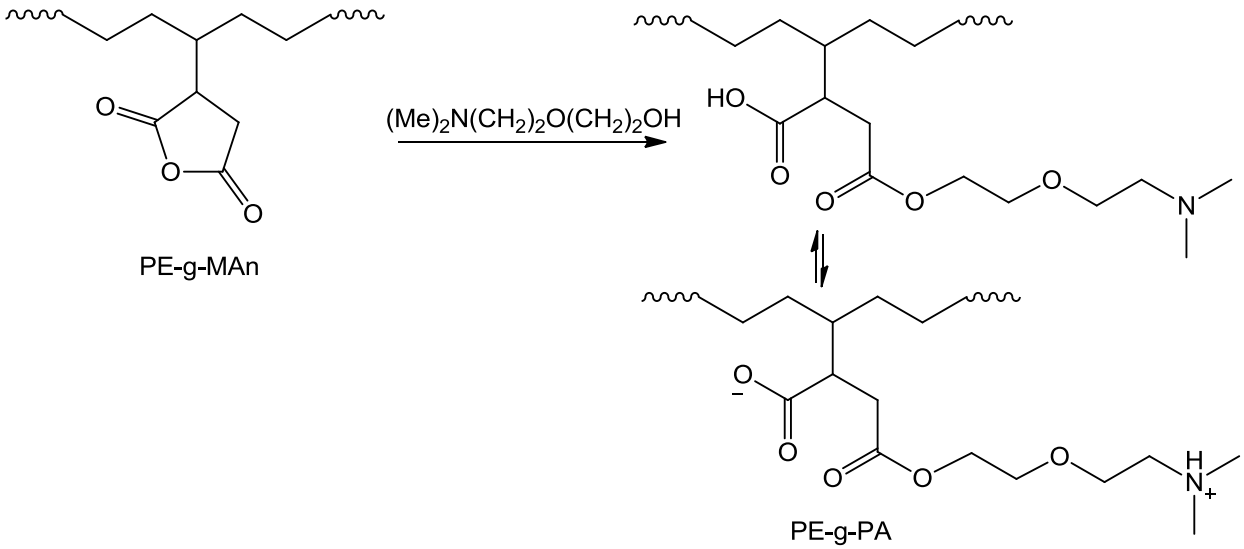

Scheme 2.4. Reaction scheme for post modification of maleated polyethylene to synthesize zwitterionic functionality.

This functionality is structurally distinct from most zwitterions. The charges are not directly linked and they are separated by 10 intervening atoms, a distance far greater than in conventional zwitterions. This reaction synthesized a stable zwitterionomer, labelled a polyethylene polyampholyte (PE-g-PA), during melt compounding as a post modification step unlike most zwitterionomers in literature which have been produced by solution based copolymerizations. Its synthesis is similar in procedure to alkylamine neutralizations of conventional ionomers however the reaction displayed an order of magnitude increase in complex viscosity and elastic modulus, changes similar to what has been reported for zwitterionomers and metal based ionomers.

The properties of these succinic anhydride derived zwitterionomers suggest a high degree of physical cross-linking between their functional groups and consequently they offer potential value in the formation of novel elastomeric ionomers and ionic compatibilizers. The reaction between DMAEE and the succinic anhydride grafts of maleated polymers offers the distinct commercial advantage of melt-state preparation and is accordingly a promising reaction in the synthesis of thermoplastic elastomers by reactive compounding.

2.5 Work Cited

[1] US3264272. E.I. Dupont de Nemours, **1966,** inv.: R. R. Watkin.

[2] R. Rees, D. Vaughan, *Polym.Prepr.* **1965**, *6*, 287.

[3] A. Eisenberg, J. Kim, *Introduction to Ionomers*, Wiley, New York 1998.

[4] M. Hara, J. Wu, A. H. Lee, *Macromolecules.* **1988**, *21*, 2214-2218.

[5] A. Eisenberg, M. Rinaudo, *Polymer Bulletin.* **1990**, *24*, 671.

[6] A. Eisenberg, *Macromolecules.* **1970**, *3*, 147-154.

[7] A. Eisenberg, B. Hird, R. B. Moore, *Macromolecules.* **1990**, *23*, 4098-4107.

[8] A. Eisenberg, M. Navratil, *Macromolecules.* **1974**, *7*, 90-94.

[9] B. P. Grady, *Polymer Engineering & Science.* **2008**, *48*, 1029.

[10] J. G. Drobny, *Handbook of Thermoplastic Elastomers*, William Andrew Publishing/Plastics Design Library 2007.

[11] US3404 I34. , E.I. Dupont de Nemours, **1968**, inv.: R. W. Rees.

[12] N. R. Legge, G. Holden, H. Schroeder, *Carl Hanser Verlag, Kolbergerstr.22, D-8000 Munchen 80, FRG, 1987.574.* **1987**.

[13] P. Antony, S. K. De, *Journal of Macromolecular Science, Part C.* **2001**, *41*, 41-77.

[14] D. J. Yarusso, S. L. Cooper, *Polymer.* **1985**, *26*, 371-378.

[15] R. Register, X. Yu, S. Cooper, *Polymer Bulletin.* **1989**, *22*, 565-571.

[16] W. Cooper, *J.Polym.Sci.* **1958**, *28*, 195-206.

[17] J. G. Van Alsten, *Macromolecules.* **1996**, *29*, 2163-2168.

[18] N. K. Tierney, R. A. Register, *Macromolecules.* **2002**, *35*, 2358-2364.

[19] D. S. Bolintineanu, M. J. Stevens, A. L. Frischknecht, *Macromolecules.* **2013**, *46*, 5381-5392.

[20] A. M. Castagna, W. Wang, K. I. Winey, J. Runt, *Macromolecules.* **2011**, *44*, 5420-5426.

[21] W. Wang, W. Liu, G. J. Tudryn, R. H. Colby, K. I. Winey, *Macromolecules.* **2010**, *43*, 4223-4229.

[22] S. A. Visser, S. L. Cooper, *Polymer.* **1992**, *33*, 920-929.

[23] A. Kanazawa, T. Ikeda, T. Endo, *J.Polym.Sci.A Polym.Chem.* **1993**, *31*, 1467-1472.

[24] B. Bauer, H. Strathmann, F. Effenberger, *Desalination.* **1990**, *79*, 125-144.

[25] M. Pasternak, T. G. Dorawala, *J.Polym.Sci.A Polym.Chem.* **1991**, *29*, 915-917.

[26] R. A. Weiss, P. K. Agarwal, R. D. Lundberg, *J Appl Polym Sci.* **1984**, *29*, 2719-2734.

[27] R. A. Weiss, P. K. Agarwal, *J Appl Polym Sci.* **1981**, *26*, 449-462.

[28] P. Smith, A. Eisenberg, *J.Polym.Sci.B Polym.Phys.* **1988**, *26*, 569-580.

[29] Z. Song, W. E. Baker, *J.Polym.Sci.A Polym.Chem.* **1992**, *30*, 1589-1600.

[30] H. Xie, D. Liu, D. Xie, *J Appl Polym Sci.* **2005**, *96*, 1398-1404.

[31] S. Wang, W. Liu, R. H. Colby, *Chem.Mater.* **2011**, *23*, 1862-1873.

[32] G. J. Tudryn, W. Liu, S. Wang, R. H. Colby, - *Macromolecules.* **2011**, *44*, 3572.

[33] L. Dulac, C. G. Bazuin, *Acta Polymerica.* **1997**, *48*, 25.

[34] J. Song, M. Hong, J. Kim, J. Yoo, J. Yu, W. Kim, *Macromolecular Research.* **2002**, *10*, 304-310.

[35] H. Xie, J. Xu, *Angew.Makromol.Chem.* **1990**, *174*, 177-187.

[36] B. H. Calhoun, R. B. Moore, *J Vinyl Addit Technol.* **1996**, *2*, 358-362.

[37] J. L. Bredas, R. R. Chance, R. Silbey, *Macromolecules.* **1988**, *21*, 1633-1639.

[38] R. G. Laughlin, *Langmuir.* **1991**, *7*, 842-847.

[39] S. Kudaibergenov, W. Jaeger, A. Laschewsky, "Polymeric Betaines: Synthesis, Characterization, and Application", in: Springer Berlin Heidelberg, 2006, p. 157-224.

[40] S. Jiang, Z. Cao, *Adv Mater.* **2010**, *22*, 920-932.

[41] A. Mathis, Y. L. Zheng, J. Galin, *Polymer.* **1991**, *32*, 3080-3085.

[42] M. Ehrmann, A. Mathis, B. Meurer, M. Scheer, J. C. Galin, *Macromolecules.* **1992**, *25*, 2253-2261.

[43] V. M. Casta, A. E. Gonzalez, J. Cardoso, O. Manero, V. M. Monroy, *J.Mater.Res.* **1990**, *5*, 654-657.

[44] M. Ehrmann, R. Muller, J. C. Galin, C. G. Bazuin, *Macromolecules.* **1993**, *26*, 4910-4918.

[45] T. A. Speckhard, K. K. S. Hwang, C. Z. Yang, W. R. Laupan, S. L. Cooper, *Journal of Macromolecular Science, Part B.* **1984**, *23*, 175-199.

[46] C. Z. Yang, K. K. S. Hwang, S. L. Cooper, *Macromolecular Chemistry.* **1983**, 184.

[47] M. Gauthier, T. Carrozzella, G. Snell, *J.Polym.Sci.B Polym.Phys.* **2002**, *40*, 2303-2312.

[48] T. Wu, F. L. Beyer, R. H. Brown, R. B. Moore, T. E. Long, *Macromolecules.* **2011**, *44*, 8056-8063.

[49] B. Immirzi, N. Lanzetta, P. Laurienzo, G. Maglio, M. Malinconico, E. Martuscelli, R. Palumbo, *Makromol.Chem.* **1987**, *188*, 951-960.

[50] J. A. Lee, M. Kontopoulou, J. S. Parent, *Polymer.* **2005**, *46*, 5040-5049.

Chapter 3

Polyampholyte derivatives of ethylene propylene rubber as an alternative to chemically cross-linked thermoplastic elastomers and thermoplastic vulcanizates

3.1 Introduction

Thermoplastic elastomers (TPEs) have the properties and performance of rubber while being processable in the melt state using conventional polymer processing equipment. This class of materials includes ethylene-propylene rubber (EPR), ethylene propylene diene terpolymers (EPDM), and various styrene-based copolymers. EPR and EPDM are commonly used in blends with polypropylene (PP) to form thermoplastic polyolefins (TPOs). These blends form the basis of compounds with excellent mechanical properties, including toughness and stiffness, especially suitable for automotive applications. [1] Dynamic vulcanization is frequently employed as a means to generate thermoplastic vulcanizate (TPV) compounds with improved mechanical properties, chemical resistance, thermal and dimensional stability, compression set, fatigue properties and melt strength. TPVs typically consist of highly cross-linked rubber particles that are finely dispersed within the thermoplastic matrix.[2-6] The properties of TPVs make them desirable in a wide array of applications involving sealing systems, automotive parts, electrical applications and other consumer goods.[2, 7] Soft touch applications of TPVs, involving a lightly cross-linked elastomer phase as a matrix are especially used in automotive interiors.[8, 9]

TPVs based on polypropylene/ethylene propylene diene rubber (PP/EPDM) have been the traditional material of choice,[10] although more recently EPRs and various polyolefin elastomers have found increased use.[11-13] Production of TPVs via peroxide-mediated cross-linking is frequently used for its ease of formulation, rapid vulcanization, high temperature resistance and good compression set properties.[10] However, when peroxide is introduced to a PP/elastomer blend, two competing reactions take place simultaneously: cross-linking of the elastomer phase and degradation of PP through β-chain scission by

abstraction of tertiary hydrogen atoms from the PP chain. The latter reaction results in a deterioration of the properties of the PP matrix, and a waste of expensive peroxides in this unwanted side reaction.[11] Multifunctional reactive compounds are commonly used as co-agents, to enhance the cross-linking efficiency and to partially counteract this effect,[14] but they come at a significant cost and can have significant and unpredictable effects on the PP structure.[15]

An alternative technique to peroxide-mediated chemical cross-linking of polyolefins utilizes polyolefin modification through the introduction of ionic functionality. Lee et al. synthesized an ammonium carboxylate polyampholyte (PE-g-PA) from maleated polyethylene (PE-g-MAn), using a very simple reaction, wherein a maleated polyolefin was reacted with an aminoalcohol to form zwitterionic functional groups.[16] This reaction resulted in a substantial increase in viscosity, even though the material did not have a measurable gel content; this effect was most likely caused by the interactions between the zwitterionic groups,[16] which resulted in the formation of physical cross-links.[17,18] Physical cross-links have been shown to improve mechanical properties in a number of ion containing elastomers based on ethylene propylene diene monomer rubber (EPDM), nitrile-butadiene rubber (NBR), styrene-butadiene rubber (SBR) and nitrile rubber (NR).[19-22]

The objective of the present research is to prepare an elastomeric polyampholyte derivative of maleated ethylene propylene rubber (EPR-g-MAn), which can be used as an alternative to peroxide curing. Blending of the resulting ethylene propylene polyampholyte (EPR-g-PA) with PP should provide a TPV that is reprocessable and recyclable, while bypassing the issue of PP degradation. The physical properties of EPR-g-PA, including rheological, thermal, mechanical and adhesive properties are compared to the parent and peroxide cured EPR-g-MAn. The morphology and mechanical properties of blends with PP are also reported.

3.2 Experimental

3.2.1 Materials

Ethylene propylene rubber with a high graft content of pendant maleic anhydride groups was obtained from DuPont Canada (EPR-g-MAn, Fusabond® MF-416D, MFI = 23g/10min at 230^{o}C). Polypropylene homopolymer (PP, Escorene® PP1042, MFR=1.9g 10min^{-1} at 230^{o}C) was supplied by ExxonMobil Chemical. Irganox B225 antioxidant was obtained from BASF. 2-[2-(dimethylamino)ethoxy]ethanol (DMAEE, 98%) and dicumyl peroxide (DCP, 98%) were used as received from Sigma-Aldrich (Oakville, Ontario). Poly(ethylene co-methacrylic acid) zinc ionomer (Surlyn® 9910, MFR=0.7g 10min^{-1} at 190^{o}C) was obtained from E.I. DuPont Company. A polyamide homopolymer, Nylon 6,6, was obtained from Invista Canada.

3.2.2 Preparation and characterization of EPR-g-PA and cross-linked EPR-g-MAn

EPR-g-MAn (40 g) and DMAEE (0.538g, 4.04 mmole) were mixed with Irganox B225 (0.08 g) in a Haake PolyLab torque rheometer that controlled a Rheomix 610p mixing chamber equipped with roller rotors at 180^{o}C for 7 minutes. The amount of DMAEE was determined based on the FT-IR spectra, which showed that this amount of DMAEE was sufficient to achieve complete conversion to the polyampholyte functionality. FT-IR spectra of the product were acquired using a Nicolet Avatar 360 E.S.P. spectrometer at a resolution of 4 cm^{-1}.

Cross-linked EPR-g-MAn (EPR-Xlink) was prepared by reacting EPR-g-MAn (40 g) with 0.15wt% DCP (0.06 g, 0.12 mmol,), which was the amount needed to match the complex viscosity of EPR-g-PA, at 180°C and 60 rpm for 7 minutes in the Haake PolyLab mixer.

The resulting materials were subjected to solvent extraction for 12 hours under reflux and dried at 130°C under vacuum to constant weight to determine the gel content, according to ASTM D2765. EPR-Xlink samples were extracted with xylene, whereas EPR-g-PA samples were extracted in a 10 vol. % solution of butanol in xylene.

The kinetics of the reaction between EPR-g-MAn and DMAEE as well as the peroxide mediated crosslinking of EPR-g-MAn were monitored by recording the evolution of the linear viscoelastic (LVE) properties as a function of time, using an Alpha Technologies Advanced Polymer Analyzer 2000 (APA 2000) oscillatory rheometer. The instrument was operated using the biconical die configuration at a temperature of 180°C, frequency of 1 Hz and arc of 3^{o}. EPR-g-MAn pellets were solution coated with DMAEE or DCP in acetone then dried at room temperature in a vacuum oven before taking measurements in the APA.

3.2.3 Blend preparation

EPR-g-MAn/PP, EPR-g-PA/PP and EPR-Xlink/PP blends containing amounts of EPR ranging from 25 to 75 wt. % were compounded in the Haake PolyLab at 180^{o}C. The blends of EPR-g-MAn and PP were prepared by simultaneous addition of the components followed by compounding for 7 minutes at 180^{o}C. Blends of EPR-g-PA and PP were prepared by simultaneously adding EPR-g-MAn, PP, and a stoichiometric amount of DMAEE, and compounding for 7 minutes at 180^{o}C. Both procedures also included the simultaneous addition of the antioxidant Irganox B225 (0.08g) before compounding. Peroxide cured TPV blends were prepared by introducing EPR-g-MAn, PP and DCP (0.15 wt. % of the respective EPR-g-MAn amount) in the batch mixer and compounding for 7 minutes, followed by the addition of the antioxidant Irganox B225 (0.08g).

3.2.4 Differential scanning calorimetry (DSC)

Thermal properties were measured using a TA Instruments Q100 DSC. The thermal history was eliminated by heating to 180°C at a rate of 10 °C min^{-1}. The sample was then cooled to -60°C at 5 °C/min and subsequently heated to 180°C at 10 °C min^{-1}. The melting temperature was determined from the second heating cycle. Percent crystallinities were estimated based on the heats of fusion, using 290 Jg^{-1} as the heat of fusion of perfectly crystalline polyethylene.

3.2.5 Scanning electron microscopy (SEM)

Blend morphologies were assessed using a JEOL JSM-840 scanning electron microscope. Samples were first hot-pressed at 180^{o}C for 1 min, then immersed in liquid nitrogen for 3 min before brittle fracture. The EPR-g-MAn elastomer phase was etched in n-heptane for 2.5 h at 60^{o}C, while the EPR-g-PA elastomer phase was etched in a mixture of n-heptane and 10 vol. % butanol. The SEM images were analyzed using the Sigma Scan Pro software to estimate the average diameters of the dispersed elastomer phase particles.

3.2.6 Rheological characterization

The LVE dynamic oscillatory properties (storage modulus, G', loss modulus, G" and complex viscosity, η*) were measured as a function of angular frequency (ω) using a Reologica ViscoTech oscillatory rheometer using 20 mm parallel plate fixtures, with a gap of 1.2 mm at 180^{o}C, under nitrogen purge. The extensional stress growth coefficient (η_E^+) was measured using a Paar Physica MCR 301 rheometer equipped with a Sentmanat Extensional Rheometer (SER) fixture from Anton Paar. Measurements were performed at 180^{o}C with Hencky strain rates ($\dot{\varepsilon}$) ranging from 0.01 s^{-1} to 5 s^{-1}. A minimum of 1 s^{-1} Hencky strain rate was used for EPR-g-MAn due to the limitation of instrument precision. The LVE stress growth coefficient was evaluated from oscillatory shear measurements.

3.2.7 Mechanical properties

Tensile properties were measured using an Instron 3369 universal tester operated at a crosshead speed of 50 mm min^{-1}. Specimens were cut with a Type V die according to ASTM D638 from 1.5 mm thick sheets, which were prepared by compression molding at 180^{o}C. Flexural tests were performed according to ISO 178 at a crosshead speed of 5 mm min^{-1}. Rectangular bars of dimensions 100 x 8.0 x 4.0 mm were produced by compression molding at 180^{o}C. Notched Izod impact tests were carried out using an Instron BLI impact tester at room temperature in accordance with ASTM D 256. Specimens with dimensions 64 x 12.7 x 3.2 mm were prepared by compression molding at 180^{o}C. A minimum of five specimens were tested for each blend for each mechanical test and the average values are reported.

3.2.8 T-peel tests

The samples used in T-peel testing were composed of three layers: a flexible substrate made of aluminum (Al), a polymer film (either EPR-g-MAn or EPR-g-PA) and a test substrate (Al, Nylon or Surlyn®). The polymers were pressed into thin films (0.12-0.15 mm) using a hot press at 250°C. The films were adhered to the aluminum substrate, at 210°C in the hot press. Subsequently the Al-polymer assembly was adhered to the test substrate in the hot press for 8 s at 210°C. Differential heating was used during adhesion to Surlyn® to avoid its deformation or melting. The Al-polymer assembly was heated to 210°C, while Surlyn® was heated to 70 °C. The initial and average peel strength were examined using Instron 3369 universal tester operated at a crosshead speed of 254 mm/min using a 180° peel test according to ASTM D903. A minimum of 10 samples were examined for each bond composition and average values were reported.

3.3 Results and Discussion

3.3.1 EPR-g-PA synthesis and rheological properties

The reaction of EPR-g-MAn with DMAEE was used to prepare the ammonium carboxylate polyampholyte (EPR-g-PA) according to Scheme 3.1.

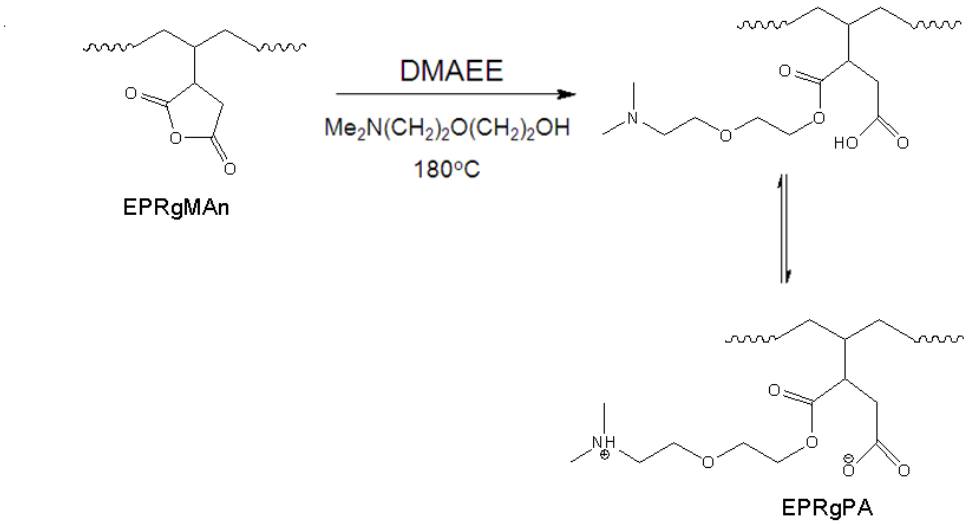

Scheme 3.1. Conversion of maleic anhydride groups of EPR-g-MAn to zwitterionic ammonium carboxylate groups in EPR-g-PA.

The completion of the reaction is confirmed by the presence of characteristic peaks attributed to the polyampholyte functionality in the FT-IR spectrum of the EPR-g-PA product. Figure 3.1 shows an intense absorbance at 1737 cm^{-1} that is characteristic of an ester along with a resonance at 1577 cm^{-1} derived from the carboxylate ion.[16]

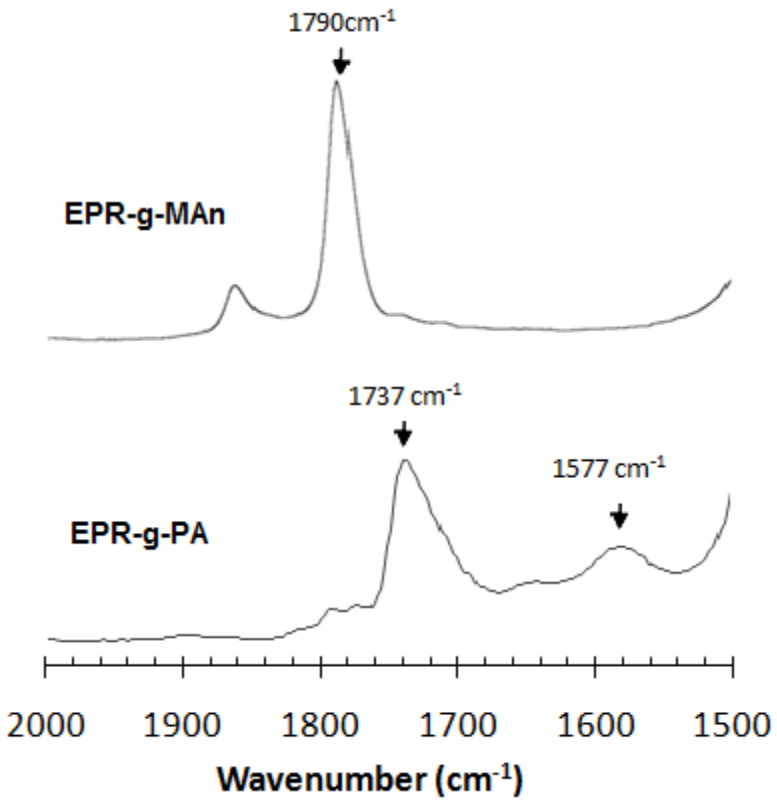

Figure 3.1. FT-IR spectra of EPR-g-MAn and EPR-g-PA.

Similar to peroxide cured polymers, which experience an increase in viscosity and modulus owing to the formation of chemical cross-links, the addition of ionic functionality to non-polar polymers alters their melt rheology because of the network effects of ion-pair aggregation.[16, 23-27] This enables us to monitor the kinetics of the reaction through simple time sweep experiments, which record the evolution of the linear viscoelastic (LVE) functions of the polymer as a function of time. The storage modulus recorded upon reacting EPR-g-MAn with DMAEE is substantially higher than the modulus of the unreacted EPR-g-MAn, as shown in Figure 3.2 a), because of the formation of a physical network. The reaction happens instantaneously upon heating the polymer within the cavity of the APA, as suggested by the immediate increase in modulus. The peroxide cured system (EPR X-link), reacted with 0.15 wt. % DCP shows a gradual increase in modulus, consistent with the time needed for decomposition of the peroxide and

completion of the reaction. This formulation achieves the same modulus after about 7 min, at 180°C. It should be noted that contrary to the DCP initiated reaction, the reaction of EPR-g-MAn with DMAEE proceeds at temperatures as low as 100°C, albeit at a slower rate, shown in Figure 3.2 b).

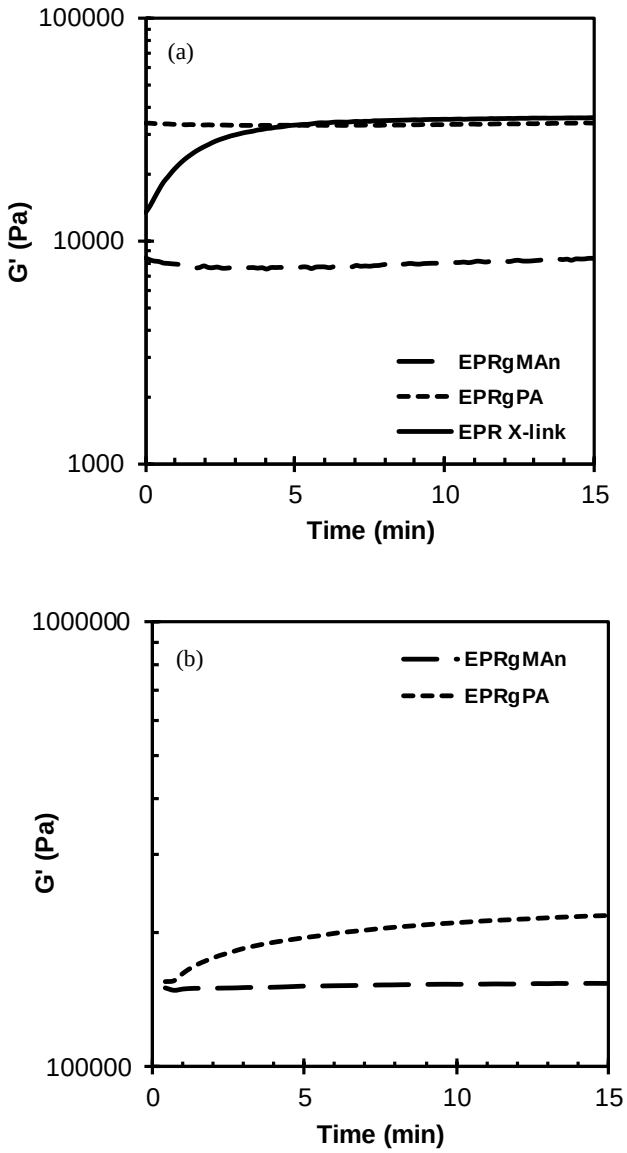

Figure 3.2. Evolution of storage modulus for the reaction of EPR-g-MAn with DMAEE in comparison with reaction of DCP with EPR-g-MAn and unreacted EPR-g-MAn at a) 180^{o}C and b) 100^{o}C.

Frequency sweeps of the final products revealed an increase of an order of magnitude in complex viscosity and storage modulus of EPR-g-PA relative to EPR-g-MAn, shown in Figure 3.3, in addition to a loss of the Newtonian plateau, and a substantial reduction in the loss tangent tanδ.

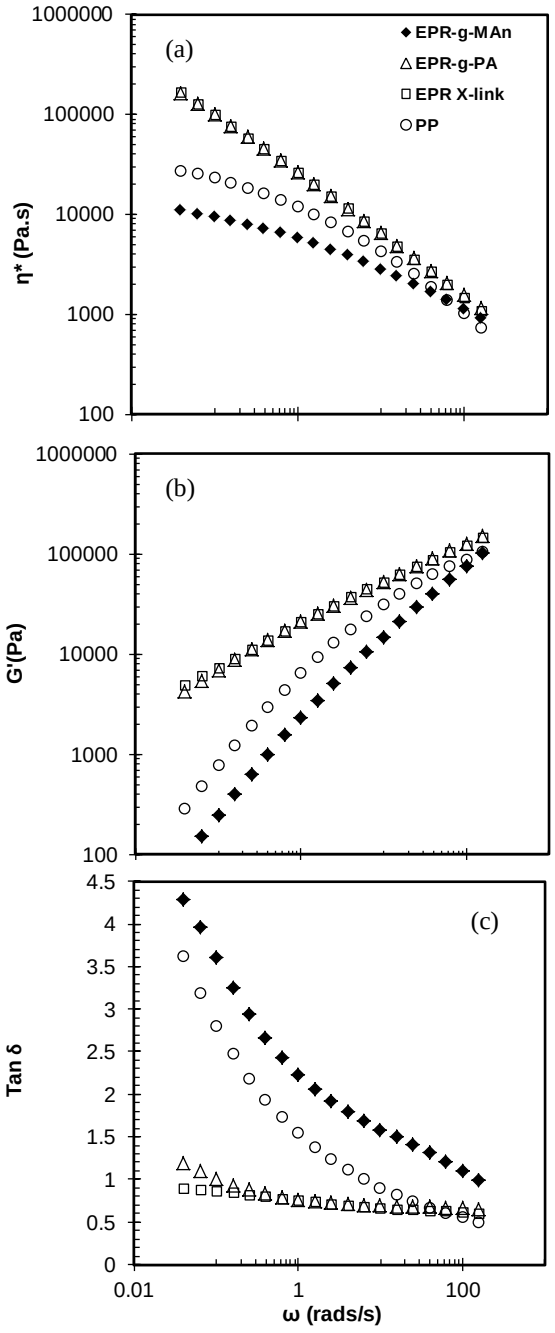

Figure 3.3. a) Complex viscosity, b) storage and c) tanδ as a function of frequency, for EPR-g-MAn, PP, at 180°C.

The melt state rheological properties of EPR-g-PA are nearly identical to those of EPR X-link over the entire range of frequencies. This indicates that the physical cross-links stemming from the ion-pair network have an effect that is equivalent to that of chemical cross-linking. Furthermore, even though many ionomers show a decrease or loss of ionic cross-linking within the melt state, [28] the ionic cross-links within EPR-g-PA are stable at temperatures above the melting point despite its low ionic content.

Even though the rheological properties of the EPR-g-PA are equivalent to those of the EPR X-link, the latter showed a high amount of gel (50 wt. % in boiling xylene), whereas EPR-g-PA had 95 wt. % gel in boiling xylenes, but was completely soluble in a mixture of 10 vol. % butanol in xylene. This result is consistent with previous findings that have demonstrated that ionomers are soluble in mixtures that contain small amounts of polar co-solvents.[29]

The presence of chemical and physical cross-linking results in significant strain hardening in uniaxial extension, for both EPR-g-PA and EPR X-link, as shown in Figure 3.4.

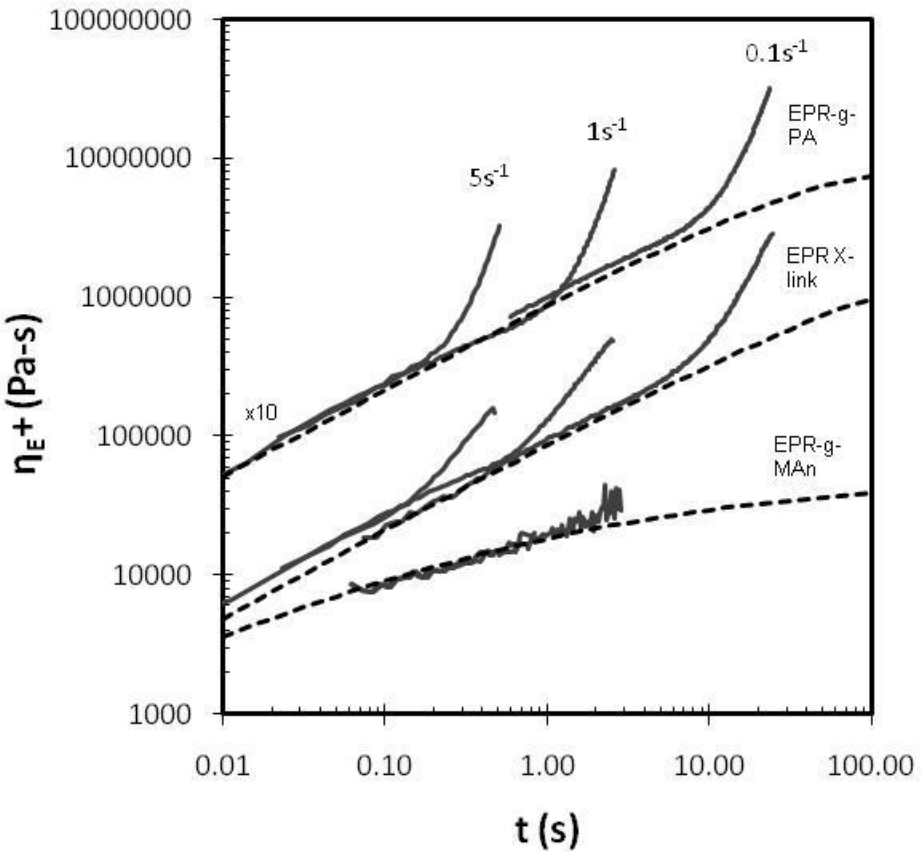

Figure 3.4. Transient extensional viscosities as a function of time for EPR-g-MAn, cross-linked EPR and EPR-g-PA at Hencky strain rates of $5s^{-1}$, $1s^{-1}$ and $0.1s^{-1}$ at 180°C. The dotted line represents the LVE stress growth coefficient calculated from the relaxation spectrum and the Trouton ratio. The EPR-g-PA curve is shifted by a factor of 10 for the sake of clarity.

EPR-g-PA shows more pronounced strain hardening at all Hecky strain rates investigated, suggesting the presence of a labile physical network. Representative values of the strain hardening coefficients, representing the ratio of the transient extensional viscosity and the Trouton ratio, at a Hecky strain rate of $5s^{-1}$ are shown in Table 3.1.

Table 3.1. Strain hardening coefficients, melting (T_m) and crystallization (T_c) temperatures and tensile properties of EPR-g-MAn, EPR-g-PA and cross-linked EPR-g-MAn.

Material	Strain Hardening Coefficient[a]	T_m(°C)	T_c(°C)	Secant modulus[b] (MPa)	Tensile Strain[c] (%)
EPR-g-MAn	1.0	29.3	23.1	1.45 ± 0.1	3040 ± 300
EPR-g-PA	8.9	34.9	18.1	2.41 ± 0.1	3452 ± 140
EPR X-link	4.0	35.1	22.2	2.40 ± 0.1	2894 ± 190

[a]Strain hardening coefficients were calculated at Hencky strains of $5s^{-1}$ and 180°C.

[b]Secant modulus was calculated at a strain of 0.25.

[c]Tensile strain at break.

These results suggest that EPR-g-PA may perform well in processes requiring high melt strength, such as thermoforming and foaming.

3.3.2 Thermal and mechanical properties

Both the EPR-g-PA and EPR-Xlink derivatives maintain the elastomeric character of EPR-g-MAn, with very low crystallinities, around 8%. The DSC heating endotherms and cooling exotherms are shown in Figure 3.5.

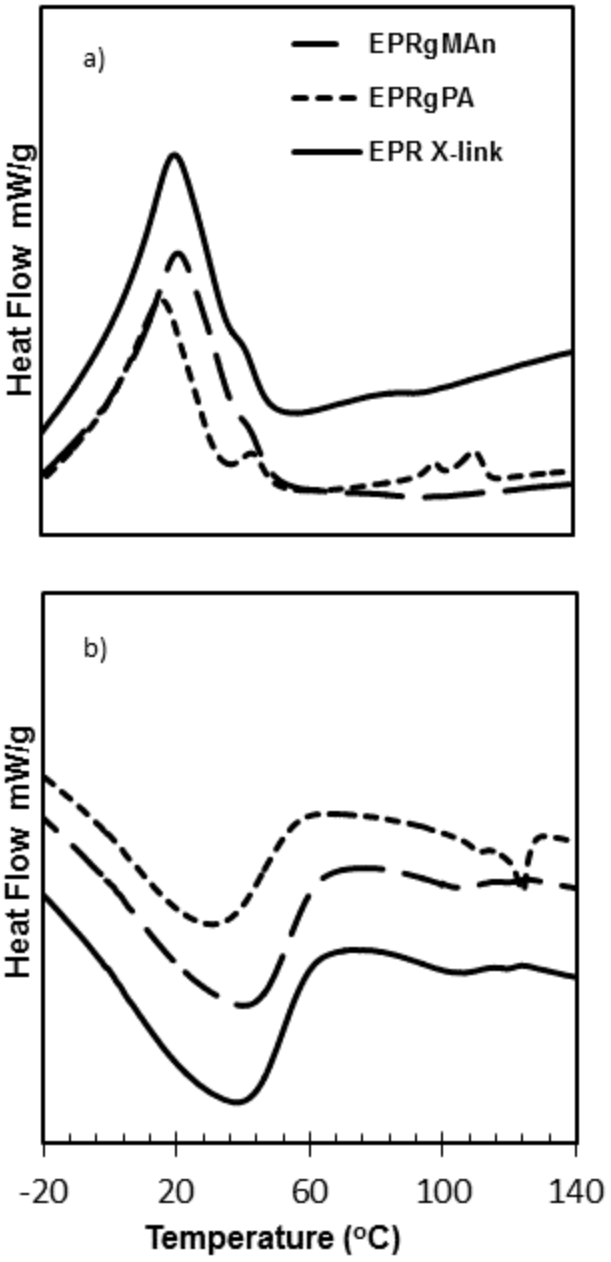

Figure 3.5. DSC a) cooling exotherm and b) heating endotherms for EPR-g-MAn, EPR-g-PA and cross-linked EPR-g-MAn.

The melting and crystallization temperatures (T_m and T_c respectively) are summarized in Table 3.1. The slight increase in T_m and decrease in T_c may be attributed to the restricted motion of the physically cross-

linked chains. The presence of minor additional peaks in the cooling exotherm at 40, 96 and 107^{o}C suggests the presence of additional crystalline forms in EPR-g-PA, similar to what has been seen in other ionomers.[30, 31]

The elastomeric properties of all materials are reflected in their low moduli and very high elongations at break, shown in Table 3.1. Both EPR-g-PA and EPR X-link show a substantial increase in secant modulus over EPR-g-MAn, however the cross-linked material experiences a decrease in elongation at break, whereas the EPR-g-PA has higher elongation, presumably due to the flexibility of the ionic networks. This result is consistent with the presence of a more labile network which was also demonstrated during the melt-state uniaxial extension tests.

3.3.3 T-peel strength

Maleated polyolefin elastomers have been used in TPV formulations because of their good adhesion characteristics, especially with polar substrates.[32] This is because the anhydride functionality improves adhesion to some metals including steel and aluminum.[33,34] The adhesive properties of the EPR-g-MAn and the EPR-g-PA materials were compared using Al, Polyamide and Surlyn® 9910, an ethylene/methacrylic acid zinc ionomer, as test substrates. The initial and average peel strengths are shown in Figure 3.6 a) and b). Given that different procedures were used for sample preparation depending on the substrate, it is only meaningful to compare the relative peel strengths between EPR-g-PA and EPR-g-MAn for a given substrate.

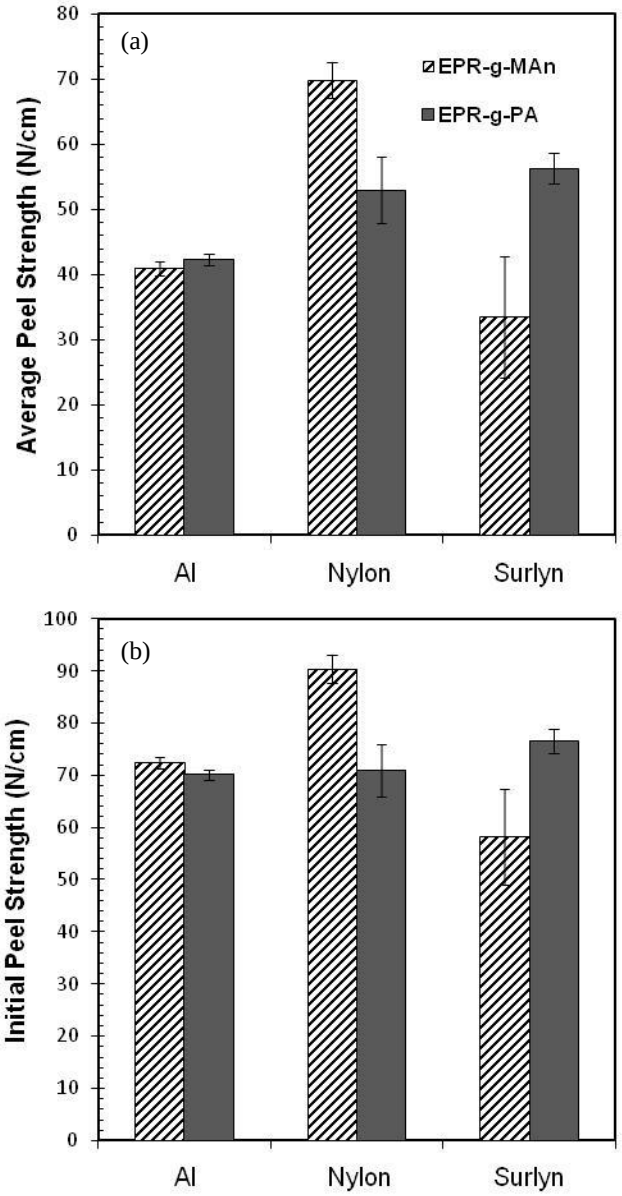

Figure 3.6. (a) Average peel strength between 20% and 80% of peel length and (b) average strength required to initiate the peel for adhesion between EPR-g-MAn or EPR-g-PA with several substrates. Average values reported in force per width (N/cm) with standard deviation.

EPR-g-MAn and its polyampholyte derivative EPR-g-PA showed similar adhesion to aluminum (Al). This suggests that the ionic interactions between the zwitterion functionality and Al compensate for the loss of covalent bonding between the maleic anhydride and aluminum oxide surface groups. The initial

and average peel strengths of the Polyamide/EPR-g-MAn/Al samples were substantially higher than those of the Polyamide/EPR-g-PA/Al samples. Furthermore in the EPR-g-MAn samples failure occurred primarily at the Al/polymer interface, whereas in the EPR-g-PA samples adhesive failure tended to occur at the polyamide/polymer interface. The lower adhesive strength of the EPR-g-PA on polyamide may be explained by the loss of covalent bonding between the amino groups and the maleic anhydride and a relatively low affinity between the amino groups and the zwitterion functionality. Conversely the initial and average peel strength of the Surlyn®/EPR-g-PA/Al samples was much higher than that of the Surlyn®/EPR-g-MAn/Al samples. Furthermore in the EPR-g-PA samples failure occurred primarily at the Al/polymer interface, while in the EPR-g-MAn samples adhesive failure occurred solely at the Surlyn®/polymer interface. This suggests that interfacial interactions are substantially stronger between the EPR-g-PA and Surlyn® compared than its maleated derivative. This may be explained by the formation of ionic multiplets during melt adhesion at the polymer interface providing strong physical interactions with the ionic functionality present within the Surlyn® ionomer.

3.3.4 EPR-g-PA/PP Blends

Representative SEM images of the blends of EPR-g-MAn/PP, EPR-g-PA/PP and cross-linked EPR-g-MAn/PP are presented in Figure 3.7. The results from the image analysis of the 25/75 wt% blend compositions are shown in Table 3.2

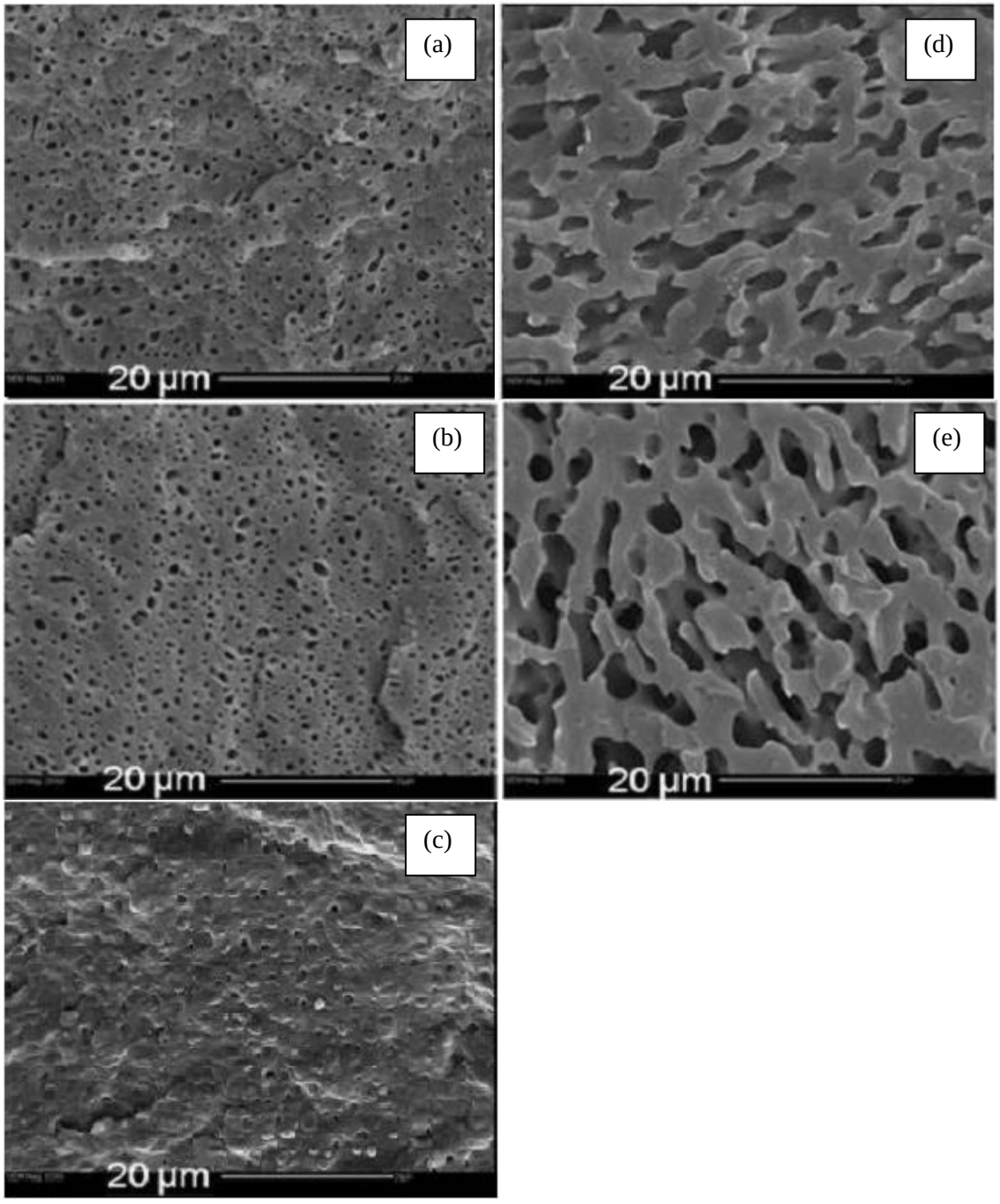

Figure 3.7. SEM images of a) 25/75 EPR-g-MAn/PP, b) 25/75 EPR-g-PA/PP, c) 25/75 EPR X-link/PP, d) 50/50 EPR-g-MAn/PP, e) 50/50 EPR-g-PA/PP .

Table 3.2. Number average diameter (d_n) and volume average diameter (d_v) with standard deviations, and polydispersity of EPR domains in PP matrix.

Blend (wt%/wt%)	d_n (μm)	d_v (μm)	Polydispersity	Viscosity Ratio*(η_{EPR}/η_{PP})
EPR-g-MAn/PP (25/75)	0.26 +/- 0.20	0.55 +/- 0.35	2.11	1.1
EPR-g-PA/PP (25/75)	0.55 +/- 0.24	0.75 +/- 0.31	1.37	1.5
EPR X-link/PP (25/75)	0.76 +/- 0.44	1.23 +/- 0.65	1.63	-

*The viscosity ratio of the blends was evaluated at frequency of 100 rad/s at 180°C. The PP viscosity in the ERP-X-link blend cannot be determined due to the unknown effect of the reaction with DCP.

The 25/75 compositions of EPR-g-MAn/PP, EPR-g-PA/PP and EPR X-link/PP have droplet-matrix morphologies with spherical EPR particles dispersed in a continuous PP matrix, while the 50/50 compositions show a morphology at the transition between droplet-matrix and co-continuous morphologies. The compositions containing EPR as the matrix phase, as well as the 50/50 EPR X-link/PP blends are not shown, because of insufficient phase contrast due to the inability to etch the dispersed phase.

While both blends have a very fine morphology with well-dispersed sub-micron size droplets, the EPR-g-MAn/PP 25/75 blend shows a slightly better dispersion, with an average droplet diameter of 0.26 μm, compared to 0.55 μm for the EPR-g-PA/PP blends. This may be attributed to the slightly higher viscosity ratio of the EPR-g-PA/PP blends (Table 3.2).[35,36] The droplet size of the 25/75 EPR X-link/PP blend cannot be assessed accurately, because of the difficulty in etching the dispersed phase. The average diameter of the dispersed droplets in this blend is slightly higher, with an average droplet size of 0.76μm.

This is likely caused by the degradation of the PP phase due to PP chain scission occurring in the presence of peroxide, resulting in decreased PP viscosity and consequently increased viscosity ratio.

In spite of their similar morphologies, the blends of EPR-g-PA/PP had substantially improved mechanical properties compared to the blends containing EPR-g-MAn and the chemically cross-linked blends, as shown in Figure 3.8, Figure 3.9 and Table 3.3 respectively.

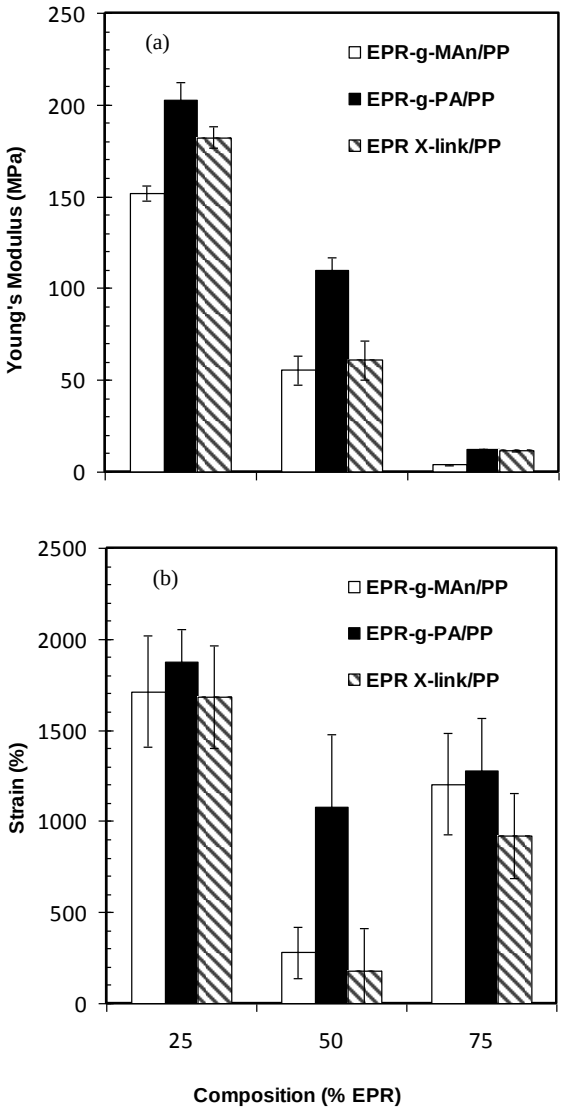

Figure 3.8. (a). Young's modulus; (b) tensile strain for blends of EPR-g-MAn/PP, EPR-g-PA/PP and EPR X-link/PP as function of composition. Values are reported with standard deviation.

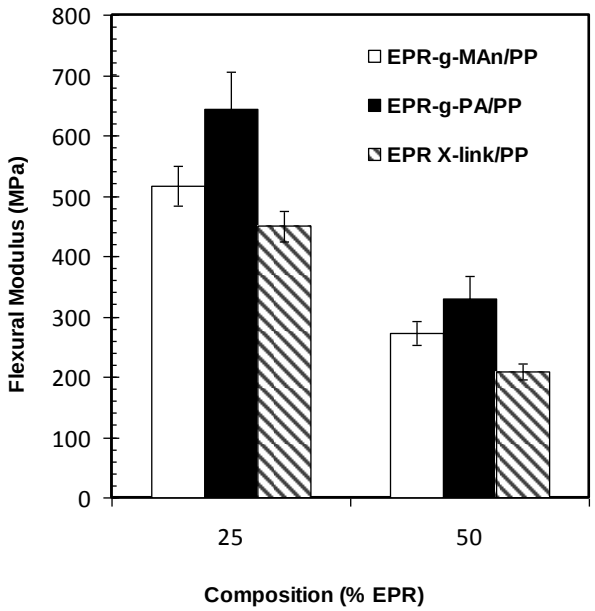

Figure 3.9. Flexural modulus for blends of EPR-g-MAn/PP, EPR-g-PA/PP and cross-linked EPR/PP for 25/75 and 50/50 compositions. Values reported with standard deviation.

Table 3.3. Impact strength for blends containing 25 wt% of EPR-g-MAn, EPR-g-PA and EPR X-link.

Blend (wt%/ wt%)	Compounding Time (min)	Impact Stength (kJ/m^2)	Break Type[a]
EPR-g-MAn/PP 25/75	7	18.3 ± 5.9	Hinged
EPR X-link/PP 25/75	7	17.8 ± 4.3	Hinged
EPR-g-PA/PP 25/75	7	26.2 ± 10.4	Mixed
EPR-g-PA/PP 25/75	4	38.9 ± 6.8	Mixed

[a]Break type indicates type of fracture upon impact. Mixed break indicates less than 90% of sample width fractured and hinged break indicates any fracture which is not complete, with 90% or more of the sample width fractured. Blends containing higher than 25% EPR did not fracture and are not included here.

This result may be due in part to the better ductility of the EPR-g-PA (Table 3.1). Additionally, peroxide cures result in unavoidable degradation of PP though β-chain scission, causing a loss of molecular weight and consequently strength. The result of the degradation reaction is evident from the rheological properties of the blends, shown in Figure 3.10 a) and b).

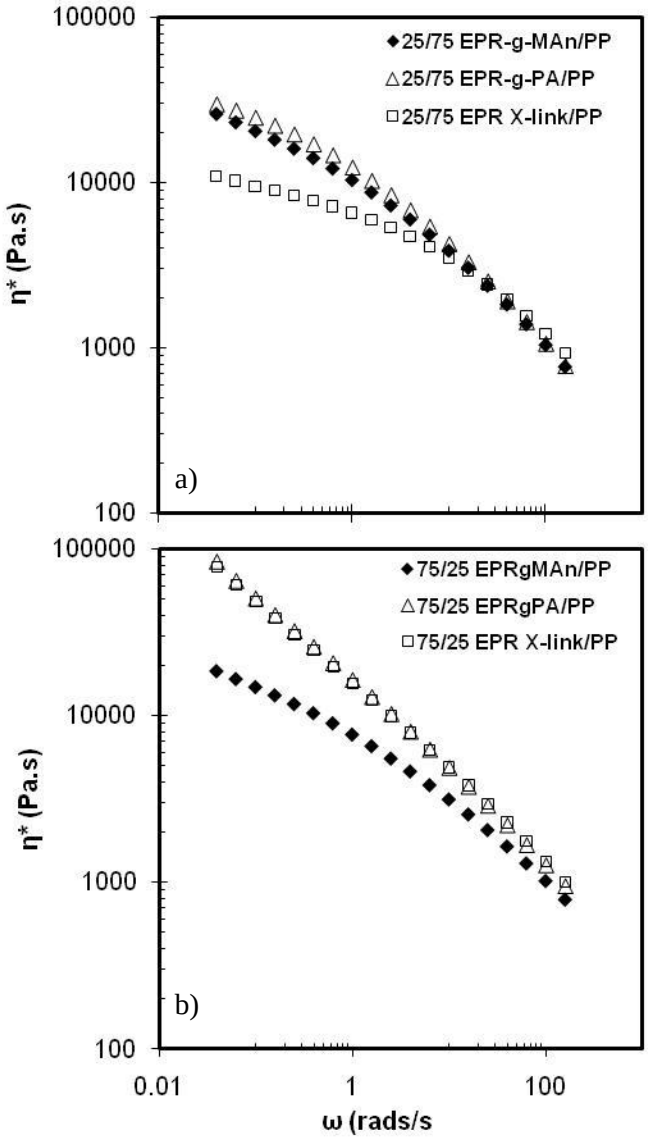

Figure 3.10. a) Complex viscosity as a function of frequency for blends of: a) 25 wt% EPR-g-MAn, EPR-g-PA and EPR X-link with 75wt% PP, b) 75 wt% EPR-g-MAn, EPR-g-PA and EPR X-link with 25wt% PP, at 180°C.

Even though the viscoelastic properties of the EPR-g-PA and the EPR X-link were identical, their blends with PP showed different properties depending on their composition. The cross-linked EPR-g-MAn/PP blends experienced a decrease in viscosity and storage modulus, particularly at higher PP compositions (Figure 3.10 a), in spite of the presence of a cross-linked component. This can be explained by the degradation of the PP phase through β-chain scission in the presence of a free radical initiator. Degradation would be especially prevalent for blends having PP as the matrix phase since more peroxide would partition within the PP phase resulting in the chain scission reaction and limiting the amount of free radicals that are available for cross-linking of the EPR phase.[11] On the contrary, the amino alcohol reacts solely with the maleic anhydride to form the zwitterion, thus retaining the PP molecular weight, while at the same time producing an elastomeric material with properties akin to the peroxide cured counterparts. This is advantageous because there is no loss of peroxide in the unwanted chain scission side reaction and the PP molecular weight remains unaffected.

It must be noted that morphology development in TPVs prepared by peroxide curing is influenced significantly by the compounding time, as well as the method for addition of peroxide,[12] due to the continuous progression of the rheological properties of the components and the need to ensure complete decomposition of the peroxide. On the contrary, as shown in Figure 2, the reaction with DMAEE is instantaneous at 180°C and the morphology development is expected to depend solely on mixing conditions. This suggests the interesting prospect that residence times can be reduced, which would be further beneficial in avoiding unwanted side reactions, such as the oxidative degradation of PP. This is evidenced by the data of Table 3.3 which shows that a reduction in the compounding time to 4 min resulted in a 48% improvement of the properties of the 25/75 EPR-g-PA/PP blends.

3.4 Conclusions

The reaction between EPR-g-MAn and amino-alcohol yielded a polyampholyte derivative with rheological properties that were similar to those of a lightly cross-linked EPR-g-MAn exhibiting high melt strength and improved tensile properties. The different surface properties of the EPR-g-PA resulted in unchanged adhesion to metals and improved adhesion to other ionomers but worse adhesion to a polyamide compared to the EPR-g-MAn.

The in-situ reaction of EPR-g-MAn with DMAEE during blending with PP produced a blend with superior impact properties compared to the blend of peroxide cross-linked EPR and PP. This is difference is attributed to the elimination of the degradation reaction of the PP phase when this chemistry is used.

These results suggest that this reaction offers a viable alternative to produce lightly cross-linked TPVs with improved strength, without suffering from the side effects of lower ductility and loss of PP strength typical of peroxide-cured systems.

3.5 Work Cited

[1] Walker B.M.,Rader C.P. (Eds.), *Handbook of thermoplastic Elastomers*, Van Nostrand Reinhold Co., New York **1988**.

[2] S. Abdou-Sabet, R. C. Puydak, C. P. Rader, *Rubber Chemistry and Technology.* **1996**, *69*, 476-494.

[3] D. Bacci, R. Marchini, M. T. Scrivani, *Polym.Eng.Sci.* **2004**, *44*, 131-140.

[4] M. D. Ellul, A. H. Tsou, W. Hu, *Polymer.* **2004**, *45*, 3351-3358.

[5] K. Naskar, *Rubber Chemistry and Technology.* **2007**, *80*, 504-519.

[6] R. Babu, N. Singha, K. Naskar, *eXPRESS Polymer Letters.* **2008**, *2*, 226-236.

[7] N. Legge, G. Holden, H. Schroeder, *Thermoplastic Elastomers: A comprehensive review*, Hanser Publishers, Munich 1987.

[8] S. Shah, N. Kakarala, *Plast.Eng.* **2000**, *56*, 51.

[9] US Pat.7294675B2. , L. P. Advanced Elastomer Systems, invs: D. Hoyweghen, A. Tonson, A. Bahar; **2007**.

[10] Naskar K., *Dynamically vulcanized PP/EPDM thermoplastic elastomers – Exploring novel routes for cross-linking with peroxides*, Ph.D. Thesis, University of Twente, The Netherlands **2004**.

[11] Z. Li, M. Kontopoulou, *Journal of Polymer Engineering.* **2011**, *26*, 633.

[12] Z. Li, M. Kontopoulou, *Polym.Eng.Sci.* **2009**, *49*, 34-43.

[13] R. R. Babu, N. K. Singha, K. Naskar, *J Appl Polym Sci.* **2009**, *113*, 1836-1852.

[14] R. R. Babu, N. K. Singha, K. Naskar, *J Appl Polym Sci*. **2009**, 113, 3207-3221.

[15] J. S. Parent, A. Bodsworth, S. S. Sengupta, M. Kontopoulou, B. I. Chaudhary, D. Poche, S. Cousteaux, *Polymer*. **2009**, *50*, 85-94.

[16] J. A. Lee, M. Kontopoulou, J. S. Parent, *Polymer*. **2005**, *46*, 5040-5049.

[17] A. Eisenberg, J. Kim, *Introduction to Ionomers*, Wiley, New York **1998**.

[18] Agarwal P. K. Agarwal, H. S. Makowski, R. D. Lundberg, *Macromolecules.* **1980**, *13*, 1679-1687.

[19] H. Makowski, R. Lundberg, L. Westerman, J. Bock, *Synthesis and Properties of Sulfonated EPDM*, American Chemical Society, **1980**, 3-19.

[20] E. E. Gilbert, *Sulfonation and related reactions.*, Interscience Publishers, New York **1965**, p. xi, 529.

[21] US Pat. 387084, Lundberg R. D., Singhal G. H., Makowski, H. S.; **1975**.

[22] T. Xavier, J. Samuel, T. Kurian, *Macromol.Mater.Eng.* **2001**, *286*, 507-512.

[23] K. Sakamoto, W. J. MacKnight, R. S. Porter, *J.Polym.Sci.A-2 Polym.Phys.* **1970**, *8*, 277-287.

[24] T. R. Earnest, W. J. Macknight, *J.Polym.Sci.Polym.Phys.Ed.* **1978**, *16*, 143-157.

[25] S. Bonotto, E. F. Bonner, *Macromolecules.* **1968**, *1*, 510-515.

[26] A. V. Tobolsky, P. F. Lyons, N. Hata, *Macromolecules.* **1968**, *1*, 515-519.

[27] A. Eisenberg, M. Navratil, *Macromolecules.* **1974**, *7*, 90-94.

[28] M. R. Tant, G. L. Wilkes, *Journal of Macromolecular Science, Part C.* **1988**, *28*, 1-63.

[29] R. D. Lundberg, H. S. Makowski, *J.Polym.Sci.Polym.Phys.Ed.* **1980**, *18*, 1821-1836.

[30] E. Hirasawa, Y. Yamamoto, K. Tadano, S. Yano, *Macromolecules.* **1989**, *22*, 2776-2780.

[31] D. J. Quiram, R. A. Register, A. J. Ryan, *Macromolecules.* **1998**, *31*, 1432-1435.

[32] K. Chatterjee, K. Naskar, *eXPRESS Polymer Letters.* **2007**, *1*, 527-534.

[33] C. Lin, W. Lee, *J Appl Polym Sci.* **1998**, *70*, 383-387.

[34] T. Funasaka, T. Ashihara, S. Maekawa, S. Ohno, M. Meguro, T. Nishino, K. Nakamae, *International Journal of Adhesion and Adhesives.* **1999**, *19*, 367-371.

[35] B. D. Favis, J. P. Chalifoux, *Polym.Eng.Sci.* **1987**, *27*, 1591-1600.

[36] P. G. Ghodgaonkar, U. Sundararaj, *Polym.Eng.Sci.* **1996**, *36*, 1656-1665.

.

Chapter 4

Zwitterionic compatibilization of polypropylene and ethylene-propylene copolymer blends

4.1 Introduction

The application of many thermoplastics is limited by their poor toughness. To mitigate this deficit thermoplastics are commonly blended with more elastic polymers, generating immiscible blends with a plastic matrix phase and elastomer dispersed phase. The presence of these dispersed rubbery particles is capable of yielding substantial improvements in mechanical properties, particularly impact strength, making blending a cost effective means of developing new polymeric materials with desired properties.[1-3]

The efficacy of the rubber-toughening of plastics is governed by blend composition, morphology and interaction between the component phases.[4-8] Interaction between phases and morphology are strongly dependent on the molecular structure of the component polymers and the blending of dissimilar polymer structures commonly leads to thermodynamically immiscible structures with high interfacial tension, low interfacial adhesion and unstable morphology.[9,10]

One means of stabilizing blend morphology is through the addition of a compatibilizer. Compatibilizers are typically heavily functionalized polymers, block copolymers or graft copolymers which are capable of strongly interacting with both phases in the blend, displaying miscibility with one phase and partial miscibility with the other.[11-13] By localizing at the phase interface compatibilizers are capable reducing interfacial tension, reducing droplet coalescence and improving adhesion between phases, thereby improving phase dispersion and mechanical properties.[14-16]

Polypropylene (PP) is commonly used in industry for its good mechanical properties, chemical resistance and low cost, however its poor impact resistance can limit its application. To improve its toughness it is commonly blended with an elastomeric ethylene-propylene random copolymer (EPR). This thermoplastic

polyolefin (TPO) blend is however morphologically unstable due to high interfacial tension and low adhesion, and the consequent coalescence of the EPR droplets may lead to a coarse morphology with reduced mechanical properties.[17]

The large differences in stereoregularity of isotactic polypropylene (i-PP) and random ethylene-propylene copolymers render these systems incompatible, so the presence of a compatibilizer is desirable to improve blend properties. Compatibilization of i-PP and EPR is however difficult due the lack of functionality in either phase, and the difficulty in synthesizing block copolymers of i-PP and EPR.[18] Several effective compatibilizers based on EP with grafted i-PP have been synthesized, though their synthesis required multistep processes involving the reaction of functionalized i-PP with functionalized EPR.[18,19]

An alternate approach, that has yet to be investigated, is the use of ionomeric EPR and PP as a means improving their phase interactions. Ionomers, polymers containing small amounts of ionic functionality grafted to their hydrocarbon backbone, are capable of forming highly exothermic interactions due to strong electrostatic forces between ionic groups forming multiplets and clusters of interacting ion-pairs.[20,21] In ionomeric polyblends, in which ion pairs form between the constituent phases, the strength of these ionic interactions between phases are evident, having been shown capable of yielding miscible blends from originally incompatible materials. [14,22] More recently, use of small amounts of ionomer has been shown to effectively compatibilize a wide range of polymer blends; improvements in phase dispersion and mechanical properties have been observed following addition of metal neutralized ethylene-methacrylic acid copolymers to blends of Nylon-6/PEVA,[23] Nylon-6/LDPE,[24] and PP/EPDM.[25]

Recent work in our laboratory has prepared an ion-containing EPR through the reaction of succinic anhydride grafted EPR (EPR-g-MAn) with dimethylaminoethoxy ethanol (DMAEE), synthesizing a zwitterionic EPR (EPR-g-PA) containing both positive and negative charge grafted to its backbone.[26] The incorporation of EPR-g-PA into i-PP was observed to substantially improve impact strength relative to blends containing the precursor EPR-g-MAn due to the elastic contributions of the ion-pair

interactions, despite exhibiting a coarser morphology. Blends of PP and EPR-g-PA may further be improved through the addition of a suitable compatibilizer. In conventional blends of PP/EPR this might require a graft copolymer of PP and EPR; however the process might be simplified by presence of the zwitterionic functionality in blends containing EPR-g-PA. A potential candidate for this application is a succinic anhydride grafted PP. This would allow for a one-pot reaction, in which the addition of DMAEE during the compounding of EPR-g-MAn, PP-g-MAn and PP could simultaneously generate zwitterionic functionality in the EPR, improving elasticity through ion-pair interactions between EPR chains, and in the PP phase, improving compatibility through ion-pair associations at the PP/EPR interface.

The present work examines the synthesis of a zwitterionic PP (PP-g-PA) from the reaction of PP-g-MAn with DMAEE and its capacity to act as an interfacial modifier in blends with EPR-g-PA and PP. This chapter investigates the synthesis and characterization of PP-g-PA and the effect of zwitterionic functionality on its properties. The focus of this chapter relates to the effect of PP-g-PA on morphology, viscoelasticity, and mechanical properties in blends of PP and EPR-g-PA with a particular emphasis on the effect of zwitterionic interactions on blend viscoelasticity. The viscoelastic properties of blends of PP-g-PA and EPR-g-PA are compared to model predictions to assist in rationalizing their behavior.

4.2 Experimental

4.2.1 Materials

Two maleated materials, an ethylene propylene rubber containing 0.5-1.0 wt% of pendant maleic anhydride groups was obtained from DuPont Canada (EPR-g-MAn, Fusabond® MF-416D, MFI = 23g/10min at 230^{o}C) and a linear isotactic polypropylene containing 0.25-0.5 wt% pendant maleic anhydride groups (PP-g-MAn, Fusabond® PMD 511D, MFR= 25g/10min at 190^{o}C). Linear isotactic PP was obtained from LyondellBasell (Pro-fax® PD702, MFR=35g/10min at 230^{o}C) to match the viscosity of the maleated PP. Irganox B225 a hindered phenol antioxidant was obtained from Ciba-Geigy. 2-[2-

(dimethylamino)ethoxy]ethanol (DMAEE, 98%) and dicumyl peroxide (DCP, 98%) were used as received from Sigma-Aldrich (Oakville, Ontario). A summary of polymers used is shown in Table 4.1.

Table 4.1. Polymer material properties.

Material	*i-PP*	*PP-g-MAn*	*EPR-g-MAn*
Trade Name	Pro-fax® PD702	Fusabond® PMD 511D	Fusabond® MF-416D
MFR (g/10min)	35@230^{o}C	25@190^{o}C	23@230^{o}C
Density (kg/m^{3})	900	900	870
Melting Point (^{o}C)	165	159	29.8
Graft Content (wt%)[a]	-	0.32	0.71

a- Graft content quantified by titration

4.2.2 Quantification of maleic anhydride graft content

Maleic anhydride content was determined using standard acid-base titration.[27,28] Prior to titration the samples were washed to extract any non-grafted maleic anhydride by dissolving 3 g of the polymer within 250 mL of toluene at reflux then precipitating the polymer from solution using acetone at room temperature.

For the titration 1g of PP-g-MAn was dissolved in 200 mL of toluene at reflux temperature. 200 uL of distilled water was added and left to react for 1 hour to hydrolyze the grafted maleic anhydride to its acid form. The hot solution was titrated with 0.010 N potassium hydroxide solution in methanol/butanol (1/9 vol/vol) using 2 drops of a 1 % solution of phenolphthalein in methanol as indicator. The titration was stopped when color remained for more than 2 min.

Color change in phenolphthalein typically occurred at a pH of 8.2, at which point both acid groups of succinic acid were fully neutralized. A MAn graft content of 0.32 wt% was calculated assuming a stoichiometric equivalent of 2.0 mol/mol. All samples remained fully soluble throughout the course of the titration.

4.2.3 Preparation of PP-g-PA

PP-g-MAn was dried in vacuum oven for 2 days at 100^{o}C to dehydrate possible succinic acid moieties to succinic anhydride. PP-g-MAn (40 g, 1.32 mmol MAn) and a 10% stoichiometric excess of DMAEE (0.193g, 1.45 mmol) with 0.2 wt% antioxidant Irganox B225 (0.08 g) were mixed in a Haake PolyLab torque rheometer that controlled a Rheomix 610p mixing chamber equipped with roller rotors at 180^{o}C for 7 minutes.

4.2.4 FT-IR analysis

Fourier transform infrared (FT-IR) spectra of the maleated and reaction products were acquired using a Vertex 70 FTIR by Burker Optics spectrometer at a resolution of 2 cm^{-1} between 400 and 4000 cm^{-1} using 24 co-added scans.

Prior to analysis samples were pressed into thin films with a thickness of approximately 100 μm by compression molding approximately 0.1g of polymer between two Teflon sheets in a Carver hydraulic hot-press at 190^{o}C.

4.2.5 Preparation of blends of PP/EPR

EPR-g-PA/PP-g-PA, EPR-g-MAn/PP-g-MAn, EPR-g-PA/PP, EPR-g-PA/PP-g-PA/PP blends containing 25 wt% EPR and 75wt% PP were prepared by a Haake PolyLab torque rheometer that controlled a Rheomix 610p mixing chamber equipped with roller rotors at 180^{o}C. All blends were prepared by the simultaneous addition of EPR-g-MAn, PP and Irganox B225 (0.08g) followed by compounding for 7 minutes at 180^{o}C, at which point a stable torque profile was observed. The preparation of blends containing EPR-g-PA and/or PP-g-PA also involved the simultaneous addition of a 10% stoichiometric excess of DMAEE. Conversion of succinic anhydride functionality to zwitterionic functionality was confirmed by FT-IR.

4.2.6 Differential scanning calorimetry (DSC)

Thermal properties were measured using a TA Instruments Q100 differential scanning calorimeter (DSC) calibrated with Indium and Zinc standards. Samples were sealed in aluminum pans and their thermal

history was erased by heating to 200°C at a rate of 10 °C/min, then holding isothermally for 5min. The sample was then cooled to -40°C at 10 °C/min and then heated to 200°C at 10 °C/min. The melting temperature (T_m), crystallization temperature (T_c) and heat of fusion (ΔH_m) were determined from the second heating cycle. ΔH_m of the PP samples were used to estimate their relative crystallinities (X_c) based on a value of 177 J/g as the heat of fusion of perfectly crystalline polypropylene.[29]

4.2.7 Scanning electron microscopy

Blend morphologies were assessed using a JEOL JSM-840 scanning electron microscope (SEM). Samples were first compression molded in a Carver hydraulic press at 190^{o}C for 1 min, cooled to room temperature then immersed in liquid nitrogen for 3 min before brittle fracture. The EPR-g-MAn elastomer phase was etched in n-heptane for 2.5 h at 60^{o}C, while the EPR-g-PA elastomer phase was etched in a mixture of n-heptane and 10 vol% butanol. The fractured surfaces were gold coated prior to imaging. The SEM images were analyzed using the software Sigma Scan Pro to estimate the average diameters of the dispersed elastomer phase particles.

4.2.8 Rheological characterization

A Carver hydraulic press, heated to 190^{o}C was used to compression mold discs approximately 2mm in thickness and 25mm in diameter. The elastic modulus (G'), viscous modulus (G'') and complex viscosity (η^*) were measured as a function of angular frequency (ω) using a Reologica ViscoTech oscillatory rheometer using 20 mm parallel plate fixtures, with a gap of 1.2 mm at 180^{o}C, under nitrogen purge.

4.2.9 Mechanical properties

Tensile properties were measured using an Instron 3369 universal tester operated at a crosshead speed of 50 mm/min. Specimens were cut with a Type V die according to ASTM D638 from 1.5 mm thick sheets, which were prepared by compression molding of the compounded samples at 180^o. Notched Izod impact tests were carried out using an Instron BLI impact tester at room temperature in accordance with ASTM D 256. Specimens with the dimensions 64 x 12.7 x 3.2 mm were prepared by compression molding at

180°C. A minimum of ten specimens were tested for each blend for the impact tests and a minimum of 7 specimens for the tensile tests and the average values were reported.

4.3 Synthesis and characterization of PP-g-PA

The melt state synthesis of a zwitterionic PP, labelled PP-g-PA, was examined by FT-IR and though reaction was expected to be equivalent to the synthesis of EPR-g-PA, a difference in reactivity of the grafted functionality was observed. This section examines the synthesis and PP-g-PA and its properties, with a comparison to its precursor PP-g-MAn.

4.3.1 Quantification of MAn graft content

Reactions involving commercial maleated polymers are complicated by the possible presence of free maleic anhydride, which in some cases has been found to be equivalent to the amount of grafted content and the lack of supplied information regarding exact graft content.[30] A maleic anhydride graft content of 0.32 ± 0.07 wt% was determined by acid-base titration using potassium hydroxide and a phenolphthalein indicator. Washing PP-g-MAn prior to analysis had a negligible effect on the calculated graft content, suggesting low levels of ungrafted MAn.

4.3.2 FT-IR analysis

FT-IR analysis of this PP-g-MAn suggested that majority of its functionality was in its succinic acid state, indicated by the broad peak at 1711cm^{-1}, similar to what was seen of EPR-g-MAn, which is typical of maleated polymers due to their susceptibility to hydrolysis.[31]

Equivalent to the procedure for the synthesis of EPR-g-PA, the reaction was performed by the simultaneous addition of the partially hydrolyzed PP-g-MAn with a stoichiometric excess of DMAEE during melt compounding at 180°C. The FT-IR spectra for the conversion of hydrolyzed PP-g-MAn to PP-g-PA are shown in Figure 4.1 spectra a) and c) respectively.

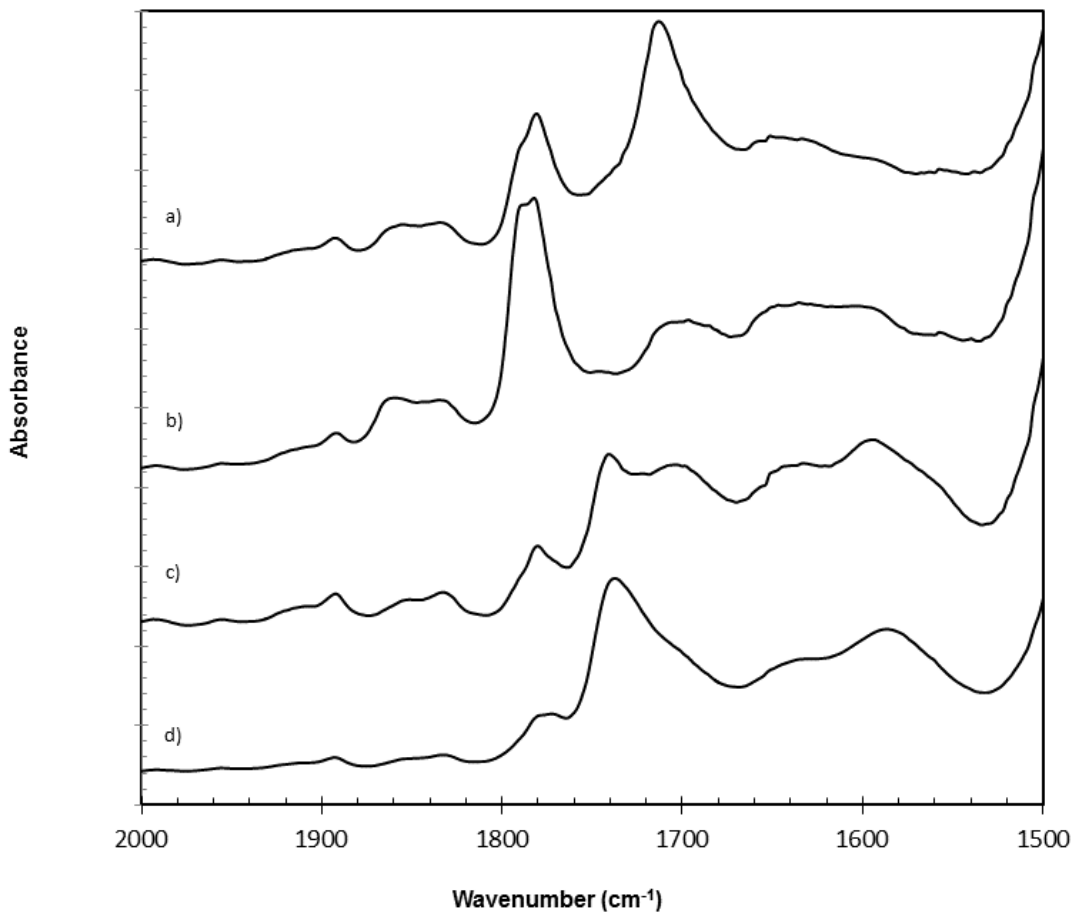

Figure 4.1. FT-IR spectra of a) partially hydrolyzed PP-g-MAn, b) dehydrated PP-g-MAn, c) PP-g-PA using partially hydrolyzed PP-g-MAn, d) PP-g-PA using dehydrated PP-g-MAn.

Following the reaction of PP-g-MAn with DMAEE FT-IR showed a large decrease in the absorbance at 1782 cm^{-1} and 1790 cm^{-1}, those originating from the succinic anhydride carbonyl groups, and the presence of a new absorbance at 1736$cm^{-1}$and 1567 cm^{-1} consistent with the reaction of the succinic anhydride carbonyl groups with DMAEE forming an ester and carboxylate anion.[26,32] A broad absorbance around 1695 cm^{-1} was also observed in the PP-g-PA spectra, which was not previously seen in the EPR-g-PA. This peak was suspected to be unreacted succinic acid however the addition of a large excess of DMAEE, 3 times the stoichiometric requirement, failed to have any further effect on conversion.

If PP-g-MAn is dehydrated prior to reacting with DMAEE the FT-IR spectra of the resulting PP-g-PA reveals an intense peak consistent with the presence of the desired ester and a large decrease in absorbance at 1695 cm^{-1} relative to the hydrolyzed PP-g-PA, shown in Figure 4.1spectra b) and d). The peak at 1695 cm^{-1} likely corresponds to the stretching vibration of carbonyl functionality of unreacted succinic acid groups and its shift to a lower wavenumber, from 1711 cm^{-1} to 1695 cm^{-1}, is likely due to hydrogen bonding with the amino alcohol, resulting in the lengthening of the C=O bond the lowering of the stretching force constant.

A quantitative determination of the conversion was difficult due to the degree of absorbance overlap and the inability to fully dehydrate PP-g-MAn however an estimate of relative conversion was possible through a comparison of the ester absorbances of the PP-g-PAs to their respective internal standards. To assist in characterizing products of the reaction of PP-g-MAn with DMAEE a comparison was made between the FT-IR spectra of partially hydrolyzed PP-g-PA and dehydrated PP-g-PA. An estimate of the relative conversion of the grafted maleic anhydride to ester functionality between two different PP-g-PA products ($PPgPA_1$ and $PPgPA_2$) was calculated from the intensity of symmetric carbonyl stretching vibration band at 1736cm^{-1} (A_{1736}) compared to the intensity of the characteristic reference absorbance of isotactic polypropylene at 1165cm^{-1} (A_{1167}) using Equation 4.1.[33]

$$\frac{[Ester_{PPgPA1}]}{[Ester_{PPgPA2}]} = \frac{A_{(PPgPA1)1736}/A_{(PPgPA1)1167}}{A_{(PPgPA2)1736}/A_{(PPgPA2)1167}} \qquad \textbf{(4.1)}$$

This comparison suggested a much larger ester concentration in the product PP-g-PA if the PP-g-MAn is dehydrated prior to reacting it with DMAEE, with a ratio of conversion of 1.64:1 for dehydrated PP-g-MAn and partially hydrolyzed PP-g-MAn respectively. Using a similar calculation at a wavelength of 1567cm^{-1} their relative carboxylate concentration was estimated to have 1:1 ratio. To rephrase this result, there is more of the ester in the dehydrated PP-g-PA relative to the partially hydrolyzed PP-g-PA however both products have an equivalent amount of the carboxylate anion. This suggests that the succinic acid groups of the partially hydrolyzed PP-g-MAn are reacting to form a carboxylate-ammonium salt rather

than forming the desired zwitterion. The likely reaction pathways for partially hydrolyzed PP-g-MAn are shown in Scheme 4.1.

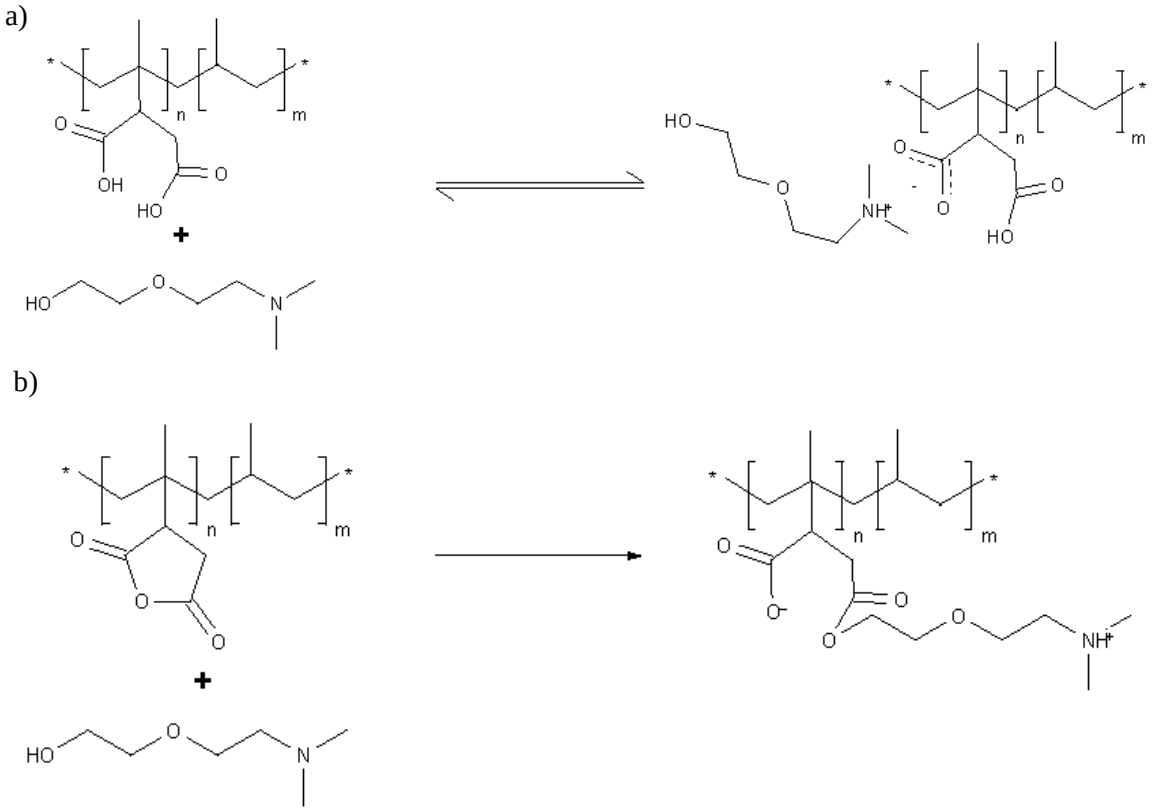

Scheme 4.1 Reaction schemes of partially hydrolyzed PP-g-MAn with DMAEE a)PP-g-MAn with succinic acid groups, b) PP-g-MAn with succinic anhydride groups. In both a) and b) the reaction might be expected to occur at both carbonyl sites of succinic anhydride, these addition pathways are excluded for simplicity.

Though the reaction of DMAEE with EPR-g-MAn and DMAEE was to found to be insensitive to the initial state of the graft functionality, the FT-IR analysis of PP-g-PA suggests the formation of the bound zwitterion when DMAEE is reacted with succinic anhydride grafts and the unbound ammonium-carboxylate complex when it is reacted with succinic acid. This difference in reactivity is difficult to rationalize considering the similarity between the reacting functional groups, though it is likely related to difficulty observed in dehydrating the hydrolyzed PP-g-MAn. While EPR-g-MAn was fully dehydrated

by melting compounding it for 7 min at 180^{o}C, it had a negligible effect on the dehydration of succinic acid groups in PP-g-MAn even for extended durations (~30min). The FT-IR of PP-g-MAn shows two anhydride peaks 1790cm^{-1} and 1782cm^{-1}, though only one is visible in EPR-g-MAn. This result is consistent with other studies of PP-g-MAn, which have attributed these two peaks to the presence of isolated anhydride grafts and closely associating intrachain anhydride groups.[30,34] The difference in reactivity might be attributed to the increased intrachain association of the diacid groups within PP-g-MAn relative to EPR-g-MAn stabilizing them by hydrogen bonding.

To avoid the complications of the diacid functionality the remainder of the work examines PP-g-PA synthesized from dehydrated PP-g-MAn. Though this was difficult to achieve quantitatively, a high degree of the anhydride could be attained by dehydrating the PP-g-MAn in a vacuum oven at 100^{O}C over 2 days at reduced pressure.

4.3.3 Thermal properties of PP-g-PA

The solid state properties of semi-crystalline polymers are dominated by their crystallinity which heavily influences their mechanical properties and thermal behavior. Crystallization in semi-crystalline ionomers, for which chains are likely participate both ionic domains and crystallites, is modified by the presence of ionic clusters. Neutralization of E/MAA and sulfonated syndiotactic polystyrene ionomers has been shown influence their crystallization kinetics and crystal structures, and is accompanied by a decrease in melting point and a substantial decrease in degree of crystallinity.[35,36]

To assess the influence of the ammonium-carboxylate zwitterionic functionality on PP crystallization the non-isothermal crystallization and melting of PP-g-MAn and PP-g-PA were examined and compared using DSC, shown in Table 4.2 and Figure 4.2.

Table 4.2. Thermal properties of PP-g-MAn and PP-g-PA: relative crystallinity (X_c), first melting peak temperature (T_{m1}), second melting peak temperature (T_{m2}), Onset temperature of crystallization (T_o), Crystallization end temperature (T_e), Peak crystallization temperature (T_p).

Sample	X_c (%)	T_{m1} (^oC)	T_{m2} (^oC)	T_o (^oC)	T_e (^oC)	T_p (^oC)
PP-g-MAn	41.8	160.0	163.7	122.8	102.8	113.2
PP-g-PA	42.0	159.3	~	130.1	106.4	115.1

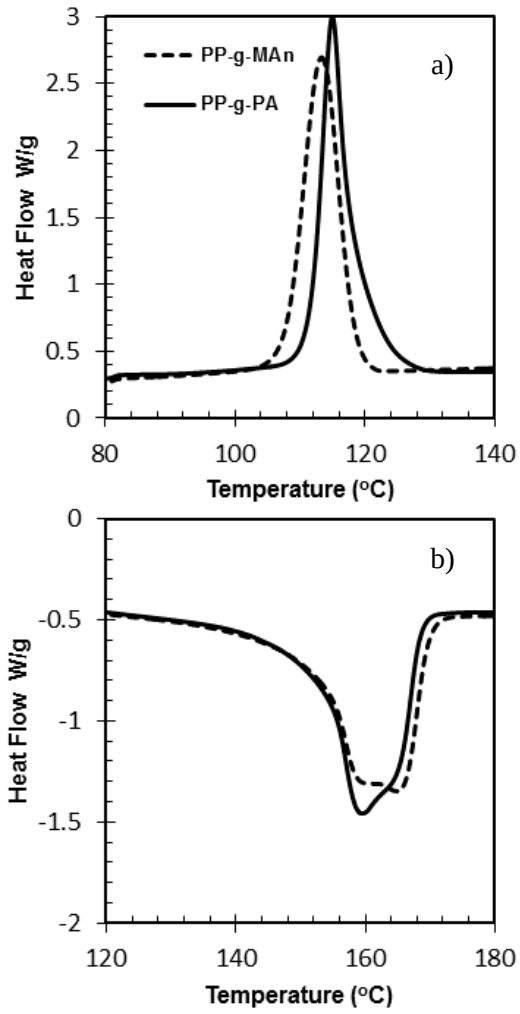

Figure 4.2. DSC spectra for PP-g-MAn and PP-g-PA: a) crystallization exotherms, b) melting endotherms

Both the maleated PP and its zwitterionomer showed similar thermal properties, with nearly equivalent crystallinities (X_c) and comparable melting points (T_m). Semi-crystalline ionomers typically exhibit large decreases in crystallinity following neutralization due to the presence of ionic clusters and their interference with lamellar ordering.[36] The similar crystallinities of PP-g-PA to PP-g-MAn may relate to the particularly low MAn graft-content, 0.3wt%, which is likely below the critical concentration for cluster formation and consequently is unlikely to substantially impede lamellar growth.

The maleated PP displayed two overlapping melting points, 160.0^{o}C and 163.7 ^{o}C, which upon conversion to PP-g-PA showed only a single melting point at 159.3^{o}C, though a shoulder near 163 ^{o}C was observed. The presence of two melting endotherms is commonly observed in low molecular weight isotactic PP, even following molecular weight fractionation.[37,38] The second endotherm has been attributed to chain reorganization and recrystallization during melting and is not present in higher molecular weight PP due its lower chain mobility.[38] The loss of the second melting peak, or its reduced prominence, in PP-g-PA is likely related to a reduction in chain mobility due to the presence of the zwitterionic interactions limiting their ability to reorganization. In literature a decrease in T_m has been observed upon neutralization in acrylic acid based semi-crystalline ionomers, and is believed to relate to the presence of ionic multiplets which may restrict the packing of chains into lamella reducing the order and thickness of the crystal structure and consequently their melting point.[39,40] This however was not observed in PP-g-PA and as previously suggested is likely related to its low ionic content.

The non-isothermal crystallization behavior of these polymers is described by the crystallization parameters: peak temperature (T_p), onset temperature (T_i) and end temperature (T_e). A particularly large difference in onset of crystallization was observed following conversion of PP-g-MAn to PP-g-PA, 130.1^{o}C and 122.8^{o}C respectively. This increase in onset temperature may be explained the presence of the zwitterionic multiplets which may act as sites for heterogeneous nucleation. Multiplets have been shown to exist in ionomer matrices substantially beyond melting temperatures which create localized areas of density and flow variations.[41] These sites can consequently act as nucleation sites, promoting a

higher onset temperature for crystallization, an effect which has been observed across a range of semi-crystalline ionomers.[41-43] It is notable that the change in onset temperature, 7.3°C, is relatively large particularly for a PP ionomer with such a low ionic concentration and comparable to what has been seen with metal based ionomers at much higher ionic concentrations. PP-g-MAn with 1.5 wt% maleic anhydride grafts neutralized with Na^+, Mg^{2+} and Ca^{2+} have been shown to have increase in onset temperature from 118 to 123°C at cooling rate of 10°C/min.[42]

An additional crystallization peak was observed in EPR-g-PA, which was believed to relate to the presence of ionic clusters,[26] however no secondary peak was observed in the zwitterionic PP. The origin of this secondary peak was unclear, and was believed to relate to a secondary crystallization. In E/MAA ionomers the presence of an additional endotherm at approximately 50°C, substantially lower than the E/MAA melting point (~95°C), has been commonly reported.[33,39,44,45] The origin of this additional endotherm has been attributed to the melting of thinner crystal structures which were reported to form over long periods of time post primary crystallization, developing over the course of several weeks in storage at room temperature.[33,44,45] This slow crystallization process was believed to occur in areas of high multiplet and cluster density in which lamellar growth was inhibited during initial crystallization. Even after 2 months at room temperature no secondary endotherm was observed in PP-g-PA. The magnitude of this effect has been shown to strongly dependent on ionic concentration, so it is possible that the lack of the secondary crystallization peak in PP-g-PA is related to its low ionic content. The origin of the secondary crystallization peak in semi-crystalline ionomers remains somewhat controversial having been attributed to cluster order-disorder transitions,[39,46] or the melting of thin crystals [33,44] and it has not been reported in PP ionomers,[42,47] so the reason for its absence in this PP zwitterionomer remains difficult to ascertain.

4.3.4 Effect of conversion of PP-g-MAn to PP-g-PA on viscoelastic properties

The dynamic viscosity-shear rate curves for PP-g-MAn and PP-g-PA are compared in Figure 4.3.

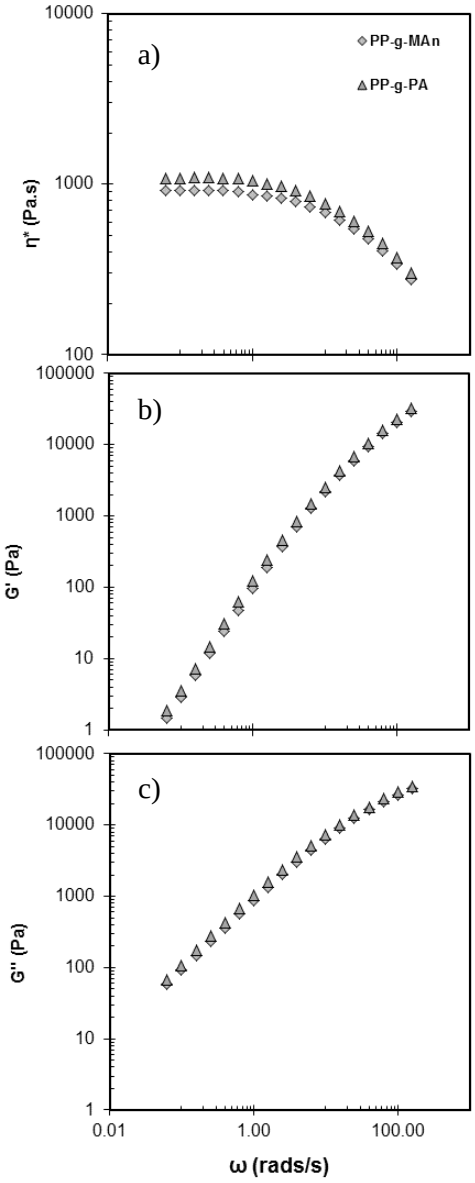

Figure 4.3. Viscoelastic properties of PP-g-MAn and PP-g-PA as a function of frequency at 180°C: a) Complex viscosity, b) Storage modulus, c) Loss Modulus.

The introduction of zwitterionic functionality showed only a marginal effect on viscoelasticity, with an increase in complex viscosity of 920 Pa.s and 1300 Pa.s and a negligible effect on modulus 0.06 rads/s. Relative to the greater-than order-of-magnitude increase in complex viscosity and storage modulus observed following the conversion of EPR-g-MAn to EPR-g-PA this effect appears particularly low. This

result is also inconsistent with the order-of-magnitude changes in viscoelasticity reported in metal-neutralized PP-acrylic acid ionomers.[48,49]

This difference in behavior may be rationalized by the low ionic content, 0.3 MAn wt% (0.13 mol%) and the low molecular weight of this maleated PP. The large changes in PP ionomer viscoelasticity in literature were reported for substantially higher ionic contents, 2-3 mol%.[48] Though the EPR-g-MAn previously examined only contained 0.7 MAn wt% its relatively large change in viscoelasticy upon neutralization is likely related to its high molecular weight. The peroxide mediated grafting of maleic anhydride onto i-PP in the melt state typically results in substantial chain degradation due to radical induced chain scission, and consequently maleated PP typically has low molecular weight.[27,50] Due to its particularly low ionic content and low molecular weight there exists relatively few functional groups per PP chain and consequently the chain network, due to the physical crosslinks between ionic groups, remains relatively small. Mechanical properties, including notched Izod impact strength and tensile results are shown in Table 4.3.

Table 4.3. Mechanical properties of PP-g-MAn and PP-g-PA at 25°C.

Composition	Young's Modulus (kJ/m^2)	Tensile Strain	Impact Strength (kJ/m^2)
PP-g-MAn	245 ± 6	882 ± 200	2.2 ± 0.4
PP-g-PA	263 ± 5	875 ± 219	2.5 ± 0.5

Similar to its rheology, the addition of the zwitterionic functional groups to PP had only small effect on mechanical properties. This similarity may be rationalized by the low functional concentration and the equivalent degree of crystallinity observed in PP-g-MAn and PP-g-PA. Given that the solid state properties of semi-crystalline polymers depend heavily on the contributions of their crystallites, the equivalent relatively crystallinities of PP-g-MAn and PP-g-PA is likely largely responsible for their

comparable properties. A similar result was observed in PP-acrylic acid ionomers, which exhibited flexural properties nearly independent of degree of neutralization.[48]

4.3.5 Conclusion

A zwitterionic PP was synthesized by reacting DMAEE with PP-g-MAn. Unlike the synthesis of EPR-g-PA, the synthesis of PP-g-PA required prior dehydration of PP-g-MAn to eliminate the diacid functionality that is commonly present to avoid the formation of unbound carboxylate-ammonium groups. The conversion of PP-g-MAn to PP-g-PA had some effect on the PP thermal behavior, with trends similar to other semi-crystalline ionomers, suggesting some interaction between the zwitterionic functional groups. The increase in the onset temperature of crystallization was indicative of heterogeneous nucleation induced by the presence of zwitterionic multiplets and is consistent with other semi-crystalline ionomers. Unlike most other ionomers, the presence of this zwitterionic functionality did not substantially affect the total crystallinity and melting point. This behavior was speculated to relate to the low ionic content of the PP-g-PA samples, though more conclusive evidence would require the study of polymers with higher MAn graft content.

Though the introduction of zwitterionic groups affected its thermal behavior it had negligible effects on mechanical properties and only marginal effect on viscoelasticity, likely due to its low zwitterionic concentration.

4.4 Zwitterionic blends of PP and EPR

Despite exhibiting similar properties to PP-g-MAn the presence of the polar zwitterionic functionality in PP-g-PA may allow it to function as an effective compatibilizer, particularly for other ionomers. Due to their similarity in structure and ease of synthesis blends of PP-g-PA and EPR-g-PA were convenient means of examining zwitterionic compatibilization. This section examines the effect of introducing zwitterionic functionality into blends of PP and EPR by examining the morphology and properties of binary blends of PP-g-PA and EPR-g-PA and blends of i-PP/ EPR-g-PA incorporating small amounts of

PP-g-PA. A particular emphasis was placed on the viscoelasticity of these blends, which were compared to model predictions to assist in rationalizing their atypical behavior.

4.4.1 Morphologies of EPR-g-PA/PP-g-PA blends

The effect of conversion of blends of EPR-g-MAn/PP-g-MAn to EPR-g-PA/PP-g-PA was examined by scanning electron microscopy (SEM). Blends were cryogenically fractured and the EPR phase was etched to facilitate image analysis. Representative SEM micrographs of blends containing EPR-g-MAn/PP-g-MAn and EPR-g-PA/PP-g-PA are shown in Figure 4.4 and image analysis of these blends is presented in Table 4.4.

Table 4.4. Number average diameter (dn) and volume average diameter (dv), and polydispersity index (dv/dn) of EPR domains in PP matrix. Viscosity ratio of blends are given at frequency of 100 rad/s at 180^{o}C.s

Blend	d_n (μm)	d_v (μm)	Polydispersity Index	Viscosity Ratio (η_{EPR}/η_{PP})
EPR-g-MAn/PP-g-MAn (25/75)	1.65	2.16	1.31	3.1
EPR-g-PA/PP-g-PA (25/75)	1.14	1.21	1.06	4.1

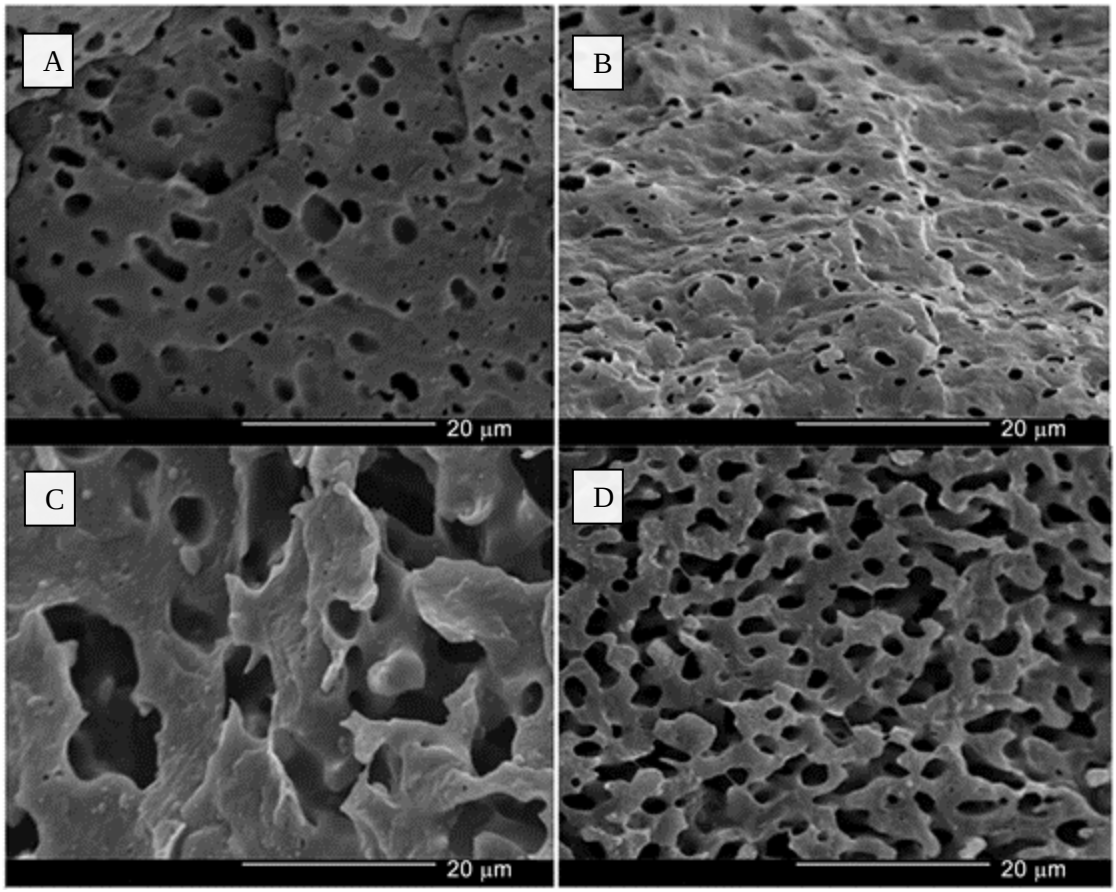

Figure 4.4. SEM images of etched blends: A) 25/75 EPR-g-MAn/PP-g-MAn, B) 25/75 EPR-g-PA/PP-g-PA, C) 50/50 EPR-g-MAn/PP-g-MAn, D) 50/50 EPR-g-PA/PP-g-PA

Each of the 25/75 EPR/PP blend compositions displayed droplet-matrix morphologies in which the minor phase, EPR, was dispersed in a PP matrix. Conversion of EPR-g-MAn/PP-g-PA to EPR-g-PA/PP-g-PA resulted in a substantial decrease in droplet diameter, from 1.64 μm to 1.14 μm and a decrease in droplet size heterogeneity, given by the decrease in polydispersity index (PDI) from 1.31 to 1.06.

At the applied compounding conditions, approximately 100 rads/s and 180^{o}C, the zwitterionic blend possessed a much greater viscosity mismatch than the maleated blend, with respective viscosity ratios of 4.1 and 3.1, due to the higher viscoelasticity of the EPR-g-PA phase. Despite this increase in the viscosity ratio, which should contribute to a coarsening of the immiscible blend,[51] the zwitterionic blend displayed a substantially finer morphology. These changes are likely related to a reduced interfacial

tension between the EPR-g-PA and PP-g-PA phases, and can be attributed to strong Coulombic interactions between their zwitterionic functional groups at the phase interface.

The difference in morphology following conversion is particularly evident in the co-continuous morphologies, shown Figure 4.4 e) and f). This particularly large difference in phase sizes likely relates to the diminished contribution of viscosity ratio on morphology in co-continuous structures, which are rather more dependent on the total effective viscosity of the blend components.[52,53] Morphological coarsening in co-continuous blends is driven by interfacial tension where decreases in co-continuous phase dimensions have been associated with decreases in interfacial tension, the presence of physical crosslinks in the dispersed phase and the presence of compatibilizer at the phase interface.[52,54,55] A combination of these effects may explain the notable difference in phase dimensions observed between the EPR-g-PA/PP-g-PA and EPR-g-MAn/PP-g-MAn co-continuous morphologies. Zwitterionic interactions between the ammonium-carboxylate groups of EPR-g-PA form physical crosslinks which are capable of stabilizing phase structure, similar to what has been observed in other co-continuous blends incorporating elastomeric polymers.[52,56] Zwitterionic interactions between PP-g-PA and EPR-g-PA at the phase interface could additionally reduce phase dimensions by supressing coalescence and reducing interfacial tension, effects which have been reported in co-continuous blends incorporating interfacial modifiers such as block copolymers and reactive compatibilizers.[54,55]

4.4.2 Comparison of viscosity of i-PP to PP-g-PA

Commercial isotactic PP-g-MAn is typically heavily degraded due to peroxide initiated chain scission during the grafting of maleic anhydride.[27,50] Due to its higher cost and limited molecular weight PP-g-MAn is typically only used as a compatibilizer and is commonly incorporated in blends containing functional polymers or fillers.[57,58] Similarly, PP-g-PA would be better suited as an interfacial modifier than as a major phase. The effect of conversion of PP/EPR maleated blend to the PP/EPR zwitterionic blend on blend morphology was somewhat confounded by the differences in blend viscosity ratios and by the presence of polar interactions and hydrogen bonding between the partially hydrolyzed MAn groups of

PP-g-MAn and EPR-g-MAn. To examine its application as an interfacial agent and to limiting the confounding effects of viscoelastic differences the compatibilizing effect of PP-g-PA was evaluated by incorporating small amounts of PP-g-PA into TPE blends of isotactic PP and the zwitterionic EPR-g-PA using non-functionalized isotactic PP of similar viscoelasticity (PD702).

A comparison of the dynamic complex viscosity of PD702 and PP-g-PA is shown in Figure 4.5.

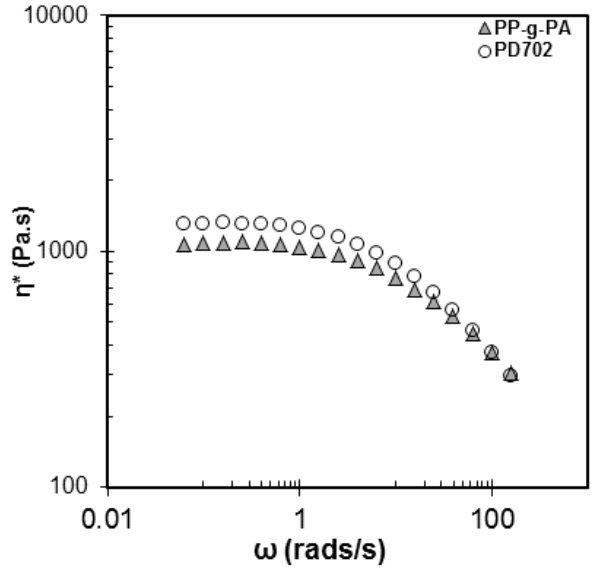

Figure 4.5. Complex viscosity as a function of frequency for PP-g-PA and PD702 at 180°C.

At compounding conditions, approximately 100 rads/s, both PD702 and PP-g-PA have nearly equivalent viscosity and moduli, making PD702 a suitable material to facilitate the study of the interfacial effect of PP-g-PA without the confounding effect of phase viscoelastic dissimilarities.

4.4.3 Effect of PP-g-PA on EPR-g-PA/PP blend morphology

Fractured and etched surfaces of 25/75 wt% EPR-g-PA/PP, in which the PP phase is composed of either PD702, PP-g-PA or a combination of PD702 and PP-g-PA are shown in Figure 4.6 and image analysis of these blends is presented in Table 4.5.

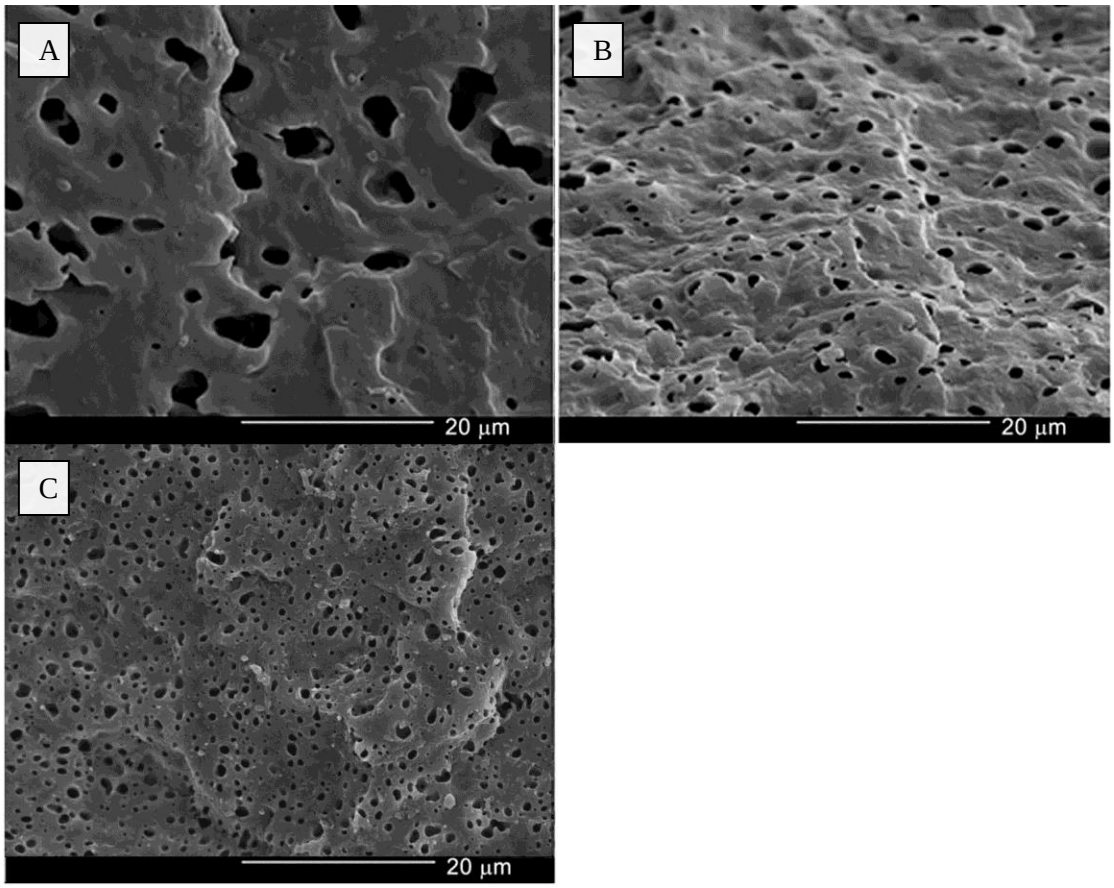

Figure 4.6. SEM images of etched blends: A) 25/75 EPR-g-PA/PD702, B) 25/75 EPR-g-PA/PP-g-PA, C) 25 EPR-g-PA/7.5 PP-g-PA/67.5 PD702

Table 4.5. Number average diameter (dn) and volume average diameter (dv) with standard deviations, and polydispersity (dv/dn) of EPR domains in PP matrix. The viscosity ratios of the blends are given at frequency of 100 rad/s at 180°C.

Blend	**d_n (µm)**	**d_v (µm)**	**Polydispersity Index (PDI)**	**Viscosity Ratio (η_{EPR}/η_{PP})**
EPR-g-PA/PD702 (25/75)	2.15	3.16	1.47	4.1
EPR-g-PA/PP-g-PA (25/75)	1.14	1.21	1.06	4.1
EPR-g-PA/PP-g-PA/PD702 (25/67.5/7.5)	0.89	1.00	1.12	4.1

A comparison of the 25/75 EPR-g-PA/PD702 and 25/75 EPR-g-PA/PP-g-PA blends showed large decrease in droplet diameter from d_n=2.15 μm to d_n=1.14 μm, and a decrease in PDI from1.47 to 1.06. These improvements in blend morphology suggest that the presence of the zwitterionic groups in PP-g-PA, despite their low concentration, is strongly affecting interfacial properties reducing interfacial tension and droplet coalescence.

Though the binary blend of PP-g-PA and EPR-g-PA suggests a reduction in interfacial tension and phase coalescence, PP-g-PA may not behave as an effective compatibilizer in blends of PP and EPR-g-PA if it fails to diffuse to the phase boundary. This might be a possible concern if PP-g-PA functional groups were to preferentially form zwitterionic multiplets and interactions with other PP-g-PA zwitterionic groups. A similar issue has been observed in long block copolymers which may form micelles within a single phase rather than migrating to the interphase during compounding.[59,60] The addition of 7.5 wt% PP-g-PA to blends of EPR-g-PA/PD702 reduced droplet diameter from d_n=2.15 μm to d_n=0.89 μm, and was accompanied by a decrease in droplet size distribution, represented by a decrease in PDI from 1.47 to 1.19. These substantial changes in blend morphology suggest that PP-g-PA was heavily localized at the phase interface rather than forming isolated multiplets in the PD702 matrix. Similar decreases in droplet sizes and improvements to dispersion have been observed in blend systems modified by conventional ionomers and reactive compatibilizers.[15,23,61,62] The morphological changes in these systems were primarily attributed to decreases in interfacial mobility due to the presence of compatibilizer chains at the interface and the suppression of droplet coalescence.

A comparison of EPR-g-PA/PP-g-PA to EPR-g-PA/PP-g-PA/PD702 morphologies reveals a finer morphology in the ternary blend. This was somewhat surprising considering the equivalent viscosity ratios at compounding conditions. The exact of cause of this difference is unclear, though it may reflect the inadequacy of the estimated 100 rad/s to express the shear conditions within the Haake batch mixer, which is likely to contain a shear gradient. At shear rates below 100 rad/s PD702 exhibits a slightly

higher viscoelasticity than PP-g-PA, shown in Figure 4.5; consequently the viscosity ratio of EPR-g-PA/PP-g-PA/PD702 might be slightly lower than that of EPR-g-PA/PP-g-PA.

4.4.4 Mechanical properties of zwitterionic blends of EPR/PP

The notched Izod Impact strength and tensile properties of the maleated, zwitterionic and compatibilized blends containing 25/75 wt% EPR/PP and their neat materials are presented in Table 4.6.

Table 4.6. Tensile and impact properties of neat materials and blends at room temperature. Errors represent the standard deviations.

Composition (wt%)	Young's Modulus (MPa)	Yield Stress (MPa)	Tensile Strain at break (%)	Impact Strength (kJ/m^2)
Neat Materials				
PP-g-MAn	245 ± 6	27.4 ± 0.2	882 ± 200	2.2 ± 0.4
PP-g-PA	263 ± 5	28.0 ± 0.3	875 ± 219	2.5 ± 0.5
PD702	236 ± 6	26.9 ± 0.3	1722 ± 282	2.9 ± 0.3
Zwitterionic and maleated blends				
EPR-g-MAn/PP-g-MAn 25/75	170 ± 7	16.3 ± 0.5	466 ± 130	4.4 ± 0.5
EPR-g-PA/PP-g-PA 25/75	169 ± 6	16.1 ± 0.2	768 ± 165	5.9 ± 0.3
Effect of PP-g-PA compatibilizer				
EPR-g-PA/PD702	164 ± 6	14.8 ± 0.5	157 ± 48	4.8 ± 0.5
EPR-g-PA/PP-g-PA/PD702 25/7.5/67.5	169 ± 5	15.6 ± 0.3	957 ± 158	8.6 ± 0.9

The addition of 25 wt% EPR to PP substantially increased impact strength for each of the blends examined. The toughening effect of dispersed elastomeric domains on PP is well understood and relates to stress transfer to the dispersed phase and the relief of volume strain by cavitation, and depends on the elasticity, dispersion and size of the elastomer inclusions and the interfacial adhesion between phases.[63-67] The zwitterionic blend was found to have a greater impact strength than the maleated blend, with impact strengths 4.4 kJ/m^2 and 5.9 kJ/m^2 respectively. This increase likely relates to changes in dispersed phase elasticity, changes in interfacial properties and differences in blend morphology. The higher elasticity of EPR-g-PA compared to EPR-g-MAn, with a secant modulus of 2.41 MPa relative to 1.45 MPa, likely improves blend toughness. The presence of zwitterionic interactions at the interface contributes to a finer morphology, observed by SEM in Figure 4.4, phase adhesion and stress-transfer during impact.

Similarly the incorporation of 7.5wt% PP zwitterionomer into the PP/EPR-g-PA blend had a dramatic effect on impact strength with an increase from 4.8 kJ/m^2 to 8.6 kJ/m^2. Examination of the EPR-g-PA/PD702 broken samples revealed limited deformation, whereas the compatibilized samples showed substantial stress-whitening in a large area surrounding the break, consistent with a more ductile behavior. This particularly large change in impact properties likely relates to the substantially finer morphology exhibited with the addition of PP-g-PA, shown in Figure 4.6.

Though Young's modulus and yield stress of blends was found to be largely independent of droplet dispersion and the presence of zwitterionic functionality large variations in elongation at break were observed. The presence of elastomer particles in PP is commonly cited to improve tensile ductility; these improvements are however reported for PPs with elongations at break between 5-90%.[68,69] For longer strains cavitation at elastomeric inclusions, due to de-bonding of the interface, may adversely affect elongation by stress concentration facilitating crack initiation.[65] This was observed in each of EPR/PP blends, exhibiting large decreases in tensile strain and premature failure.

Poor tensile elongation was particularly notable in the EPR-g-PA/PD702 blend, having a strain of only 157% and failing prior to any observed yielding. The incorporation of 7.5 wt% PP-g-PA into this blend substantially improved ductility, exhibiting a strain at break of 957%. This increase likely relates to the improvement in phase adhesion reducing de-bonding during strain and the decrease in particle size, which is believed to diminish cavitation.[63] A greater elongation was also observed in EPR-g-PA/PP-g-PA relative to EPR-g-MAn/PP-g-MAn, with strains of 768% and 466% respectively, which may similarly be rationalized by presence of zwitterionic interactions at the phase interface, increasing dispersion and interfacial adhesion.

4.4.5 Viscoelasticity of zwitterionic blends of PP and EPR

The addition of PP-g-PA to blends of PP and EPR-g-PA improved impact properties and droplet dispersion. This may suggest the presence of strong interactions between the zwitterionic groups of PP-g-PA and EPR-g-PA at the interface of the dispersed phase improving compatibility. There is little literature on zwitterionomers and less on zwitterionic compatibilizers, so how they improve phase compatibility and their effect on blend viscoelastic properties is unknown. Viscoelastic properties of blends containing PP-g-PA and EPR-g-PA were further examined by dynamic oscillatory shear rheology to offer a better indication of the type and strength of interactions that are present between the zwitterionic groups between phases. Dynamic rheology assesses the frequency dependence of melt state viscoelastic properties and may further provide information of the blends interfacial characteristics when used in combination with their microstructural data and emulsion models. The following section examines the linear rheology of blends of PP-g-PA and EPR-g-PA and blends of PP/EPR-g-PA compatibilized with PP-g-PA with a focus on rationalizing how the zwitterionic interactions affect blend viscoelasticity.

4.4.5.1 Viscoelasticity of EPR-g-PA/PP-g-PA

The linear viscoelastic properties of the maleated and zwitterionic derivatives and their blends are summarized in Figure 4.7.

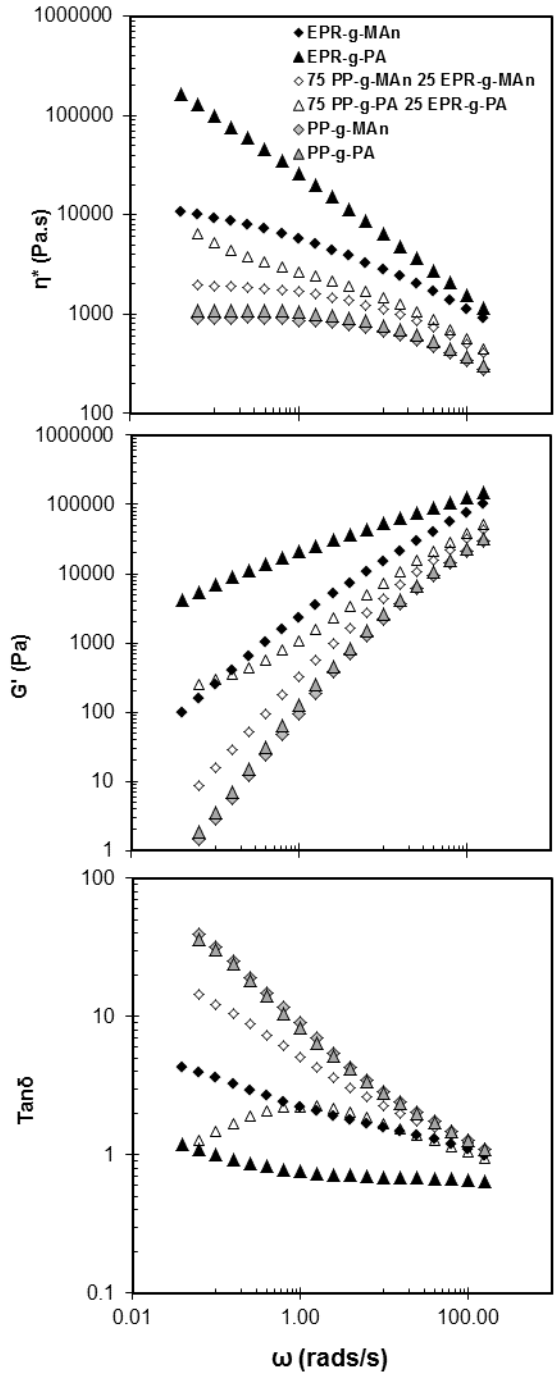

Figure 4.7. Complex viscosity, b) Storage modulus and c) Phase angle, as a function of frequency for EPR-g-MAn, EPR-g-PA, PP-g-MAn, PP-g-PA and 75/25 blends of PP-g-PA/EPR-g-PA and PP-g-MAn/EPR-g-MAn at 180oC.

The maleated blend displayed the expected rheological behavior of an immiscible blend with droplet-matrix morphology. Blend viscoelastic properties were similar to the PP matrix, displaying evident liquid-like terminal flow behavior, including a Newtonian plateau and terminal zone ($G'(\omega) \propto \omega^2$, $G''(\omega) \propto \omega$) at low frequencies.

The zwitterionic blend displayed low frequency rheological behavior that deviated substantially from Newtonian liquid emulsions, and was dissimilar from both the PP-g-MAn/EPR-g-MAn blend and the PP1042/EPR-g-PA blends discussed previously.[26]

This zwitterionic blend exhibited an inflection point in modulus and viscosity at approximately 2 rads/s corresponding to the start of the terminal zone for the polypropylene matrix. This deviation from the terminal flow behaviour of $G'(\omega) \propto \omega^2$, however was not observed in G'' scaling behavior which remained relatively unaffected, consequently this effect is also reflected in the tanδ values, which show a semi-circular shape, similar to what is generally observed in polymers that exhibit a transition from viscoelastic liquid to viscoelastic solid behaviour.

Similar rheological deviations from the terminal behavior of the matrix polymer have been previously reported in a number of immiscible blends, the cause of which has been described as a droplet distortion phenomenon.[70-72] The rheological properties of immiscible polymer blends, particularly at low frequencies, are strongly dependent on the energy storage properties of the phase interface. The effect observed with the zwitterionic blend, which displayed an enhanced elastic response at low frequencies likely relates to the relaxation of droplets deformed during shearing as a response to minimize interfacial area and is governed by the difference in relaxation time of the droplet and matrix polymers. The observed effect is that of increased contributions to storage modulus at low frequencies with a negligible effect on the loss modulus, which may give rise to decrease in tanδ, similar to what was observed in the results of the PA blends.

Droplet relaxation times are characterized by the capillary number, Rn_m/T.[72,73] Longer relaxation times, corresponding to large droplet sizes and low interfacial tensions are more likely to induce this phenomenon. Though the PA blends were found to have smaller elastomeric inclusions than the maleated blends it was speculated that these blends should have a substantially lower interfacial tension than the maleated blends due to the electrostatic interactions between zwitterionic groups, which might explain the blend's particularly large elastic response at low frequencies.

This effect is consistent with morphological observations and suggests a capacity of the zwitterionic PP to compatibilize PP/EPR-g-PA blends by reducing interfacial tension. Blend interfacial tensions may be calculated using the Palierne emulsion model for viscoelastic materials, which may assist to rationalize the difference in properties between PP-g-PA/EPR-g-PA and PP-g-MAn/EPR-g-MAn blends.

4.4.5.2 Comparison of blend viscoelasticity with Palierne model predictions

The emulsion model by Palierne accounts for the linear viscoelastic behavior of blends in which viscoelastic inclusions are dispersed within a viscoelastic matrix and has been successfully employed to predict the rheological response of a wide range of blend systems, based on the size of the domains of the dispersed phase and their interfacial tension.[70,71,74] The Palierne model has also been shown to successfully estimate interfacial tensions of binary immiscible blends using their morphological and rheological data.[74-76]

The successful application of the Palierne model should yield an estimate of interfacial tension which will contribute to understanding how the zwitterionic groups interact in the blend and assist in rationalizing the mechanical and morphological differences between the maleated and zwitterionic blends. The successful modeling of blend viscoelastic properties (G' and G'') will additionally support the presence of droplet distortion and relaxation as the origin of the low frequency behavior observed in the zwitterionic blend.

Palierne model maintains several assumptions which need be observed to maintain its applicability. A fundamental assumption of the Palierne model is that emulsion displays linear viscoelasticity;

consequently its comparison to experimental data is only applicable if the blend rheology is maintained in the linear range.[73] This was achieved by maintaining low strain amplitudes during oscillatory shear. Though the Palierne model was originally derived for a particle size distribution Bousmina and Muller showed that volume average diameter accounts for particle size distribution effects when the polydispersity index is less than two.[74,77] This simplified model is expressed in Equations 4.2 and 4.3.

$$\boldsymbol{G^*(\omega) = G^*_m(\omega)\frac{1+3\varphi H(\omega)}{1-2\varphi H(\omega)}} \qquad \textbf{(4.2)}$$

$$\boldsymbol{H(\omega) = \frac{(4\Gamma^\circ/R)(2G^*_m+5G^*_d)+(G^*_d-G^*_m)(16G^*_m+19G^*_d)}{(40\Gamma^\circ/R)(G^*_m+G^*_d)+(2G^*_d+3G^*_m)(16G^*_m+19G^*_d)}} \qquad \textbf{(4.3)}$$

φ is the polymer volume fraction in the blend

Γ° is equilibrium interfacial tension

$G^*(\omega)$ is the blend complex modulus

G^*_m is the frequency dependent complex modulus of matrix polymer

G^*_d is the frequency dependent complex modulus of dispersed polymer

R is the inclusion radius in the blend

This model was fit against the frequency profiles of the blends 75/25 PP-g-MAn/EPR-g-MAn and 75/25 PP-g-PA/EPR-g-PA using their known volume average diameters d_v(MAn)=2.16μm and d_v(PA)=1.49μm, which were determined from the image analysis of the SEM images, as parameter inputs. The equilibrium interfacial tension was determined by regression, fitting the model blend moduli to the experimental moduli. Figure 4.8 presents the elastic and storage moduli of the maleated polymers, PP-g-MAn and EPR-g-MAn, as well as the 75/25 PP-g-MAn/EPR-g-MAn blend with model predictions.

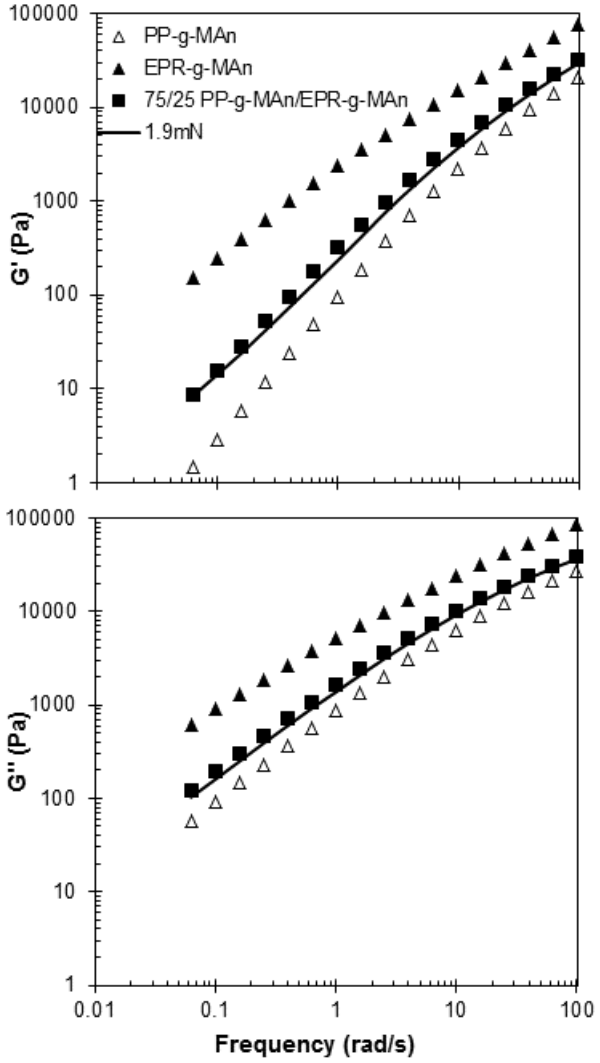

Figure 4.8. Palierne model predictions of elastic and viscous modulus as a function of frequency for 75/25 PP-g-MAn/EPR-g-MAn at 180°C, where Γ°=1.9mN/m.

The dynamic rheology of the maleated blend is consistent with Palierne's emulsion model for viscoelastic materials, where an interfacial tension of 1.9mN/m at 180°C as determined by least squares, provides a good fit. This value of interfacial tension is reasonable and similar to other estimates of interfacial tension between PP and EPR.[78]

Figure 4.9 shows the Palierne model predictions for the frequency dependence of the dynamic moduli of the 25/75 PP-g-PA/EPR-g-PA blend and their comparison to experimental values. This figure includes

model predictions for range of interfacial tensions with values: 0.35mN/m, determined by method of least squares relative to experimental data, 0mN/m and 1000 mN/m for the sake of comparison.

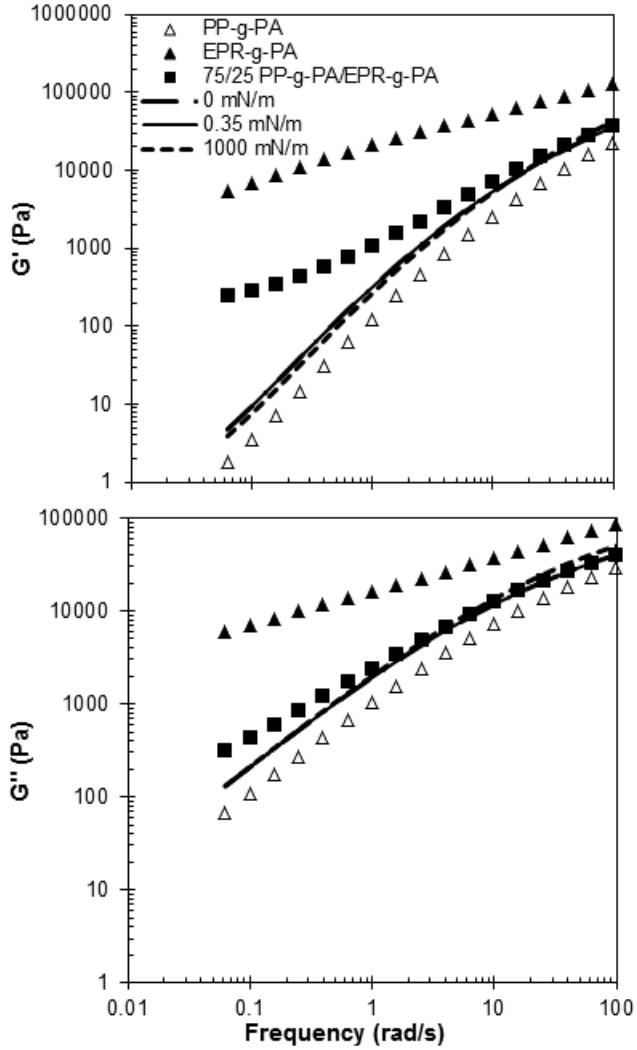

Figure 4.9. Palierne model predictions of elastic and viscous modulus as a function of frequency for 75/25 PP-g-PA/EPR-g-PA for 3 values of interfacial tension: 0 mN/m, 0.3 mN/m, 1000 mN/m at 180^{o}C.

Unlike the maleated blend the zwitterionic blend behaviour cannot be predicted by the Palierne model.

Deformation and relaxation of the shape of the dispersed droplets is accounted for in Palierne's emulsion model, including its simplified version, in which changes in droplet shape give rise to elasticity as a result of changes in interfacial area.[72,74,77]

Considering that the estimated G' curves across a range of interfacial tensions fail to predict the observed plateau it is unlikely that the EPR-g-PA droplet deformation and relaxation are directly responsible for the low frequency behavior in the zwitterionic blend as originally predicted. Though the frequency dependence of the moduli are similar to what been reported in other immiscible blends,[70-72] the basis of this behavior is likely somewhat different.

A notable observation in Figure 3 is the insensitivity of the model predictions to changes in inputted interfacial tension. The model was similarly insensitive to changes in inclusion radius. This result is likely due to the large relative difference in modulus between the droplets and matrix phase. The complex modulus of EPR-g-PA is approximately 3 orders of magnitude larger than PP-g-PA at low frequency (0.2 rads/s); the terms on the right hand side of Equation 4.3, particularly the G^2 term, are large relative to the terms involving interfacial tension and droplet radius, consequently interfacial tension and droplet radius have a negligible effect on model predictions.

Due to the large differences in melt viscoelasticity between the matrix polymer (PP-g-PA) and the dispersed phase (EPR-g-PA) the shear stresses imposed by the matrix on the elastomer droplets are unlikely to cause much deformation. Consequently, relative to the PP matrix the elastomer inclusions are likely to behave like hard un-deformable particles. PP-g-PA/EPR-g-PA blend rheology might be more similar to composite behavior for which Palierne's model is unsuited.

Similar dynamic behavior, including lack of a Newtonian plateau, presence of low frequency G' plateau and semi-circular tanδ have been reported in particle filled systems such composites and TPVs. In these systems these low frequency elastic responses have been attributed to the presence network-like structures typically through direct contact between particles within the matrix or the direct bridging of polymer

chains between particles. Aranguren et al. observed low frequency plateaus in silica systems in which the silica fused into clusters and agglomerated into a three dimensional network.[79]

Similarly blends of EPDM/PP containing have shown large deviations of elastic modulus from terminal flow at low frequencies.[80] TEMs of their blend morphologies showed evidence of contact between adjacent elastomer inclusions and the presence of an elastomer network. Bousmina and Muller have studied this effect in detail in plastic/rubber blends and concluded that this effect was related to the formation of a three dimension network of rubber particles and that the magnitude of the plateau in storage modulus was strongly dependent on degree of contact between the rubber particles.[77,81,82]

Though the PP-g-PA/EPR-g-PA blend exhibits viscoelastic properties similar to what has been observed in composites and TPVs containing networked particles, the imaging of this zwitterionic blend shows no morphological evidence to support the presence of an elastomer network of particles. The morphology of PP-g-PA/EPR-g-PA, shown in Figure 4.4, appears well dispersed, with an average interparticle separation of 1.5 um. Network formation and interparticle contact during shearing is also unlikely. Unlike filler particles and chemically cross-linked rubber, EPR-g-PA maintains its thermoplasticity at the conditions tested and would consequently be expected to coalesce if droplets were to come into contact with one another during shearing rather than form networked structures.

The failure of the simplified Palierne model to adequately describe this blend's rheology likely suggests the failure of one or more of its assumptions, and while similar results have been observed in TPVs and composites the thermoplastic nature of the zwitterionic blend and its morphology make it difficult to justify the presence of an elastomer network in the PP-g-PA/EPR-g-PA blend.

The Palierne model is invalid for large localized differences in shear which might be present in the zwitterionic blend if there are large variations in flow fields surrounding the EPR-g-PA droplets. Bousmina and Muller related the presence of the low frequency G' plateau observed during dynamic rheology to the percolation of the matrix phase through an elastomer network.[81] Immobilization of PP-g-PA chains at the EPR-g-PA surface due zwitterionic interactions may substantially alter polymer

mobility surrounding the elastomer inclusions and generate a similar percolating network without the morphological evidence of an elastomeric network. An area of low mobility surrounding the elastomer droplets may behave sufficiently different from matrix phase to exhibit its own form relaxation period similar to what has been observed in ternary blends.[83] These interface mobility related effects may contribute to the observed increase in elasticity at low frequencies and the failure of the Palierne model.

This effect might also be explained by long range interactions across the zwitterionic matrix phase. The model assumption, which maintains that the motion of the dispersed droplets is independent, may not be valid if strong associations between the zwitterionic groups within the PP-g-PA matrix bridge the EPR-g-PA droplets. This bridging of the elastomer droplets might form a three-dimensional network amplifying elastic contributions at low frequency, similar to the network effect observed in other elastomer/polyolefin blends.

4.4.6 Viscoelastic properties of ternary blends of EPR-g-PA/PP-g-PA/PP

A plateau of the storage modulus and a transition to solid-like behavior was observed in the zwitterionic blend at low frequencies, and though this effect is believed to relate to the presence of the zwitterionic groups at the droplet interface the rationale was confounded by the possibility that the behavior might also relate to the difference between matrix and dispersed phase viscosity and possibility of zwitterionic associations across the PP-g-PA matrix bridging adjacent elastomer inclusions. This viscoelasticity of ternary blends of PP/PP-g-PA/EPR-g-PA was examined to study the effect of PP-g-PA on PP/EPR-g-PA phase compatibility and assist in rationalizing this low frequency elasticity.

Figure 4.10 shows the shear rate dependence of the viscoelastic properties for blends of PP and EPR-g-PA compatibilized by PP-g-PA.

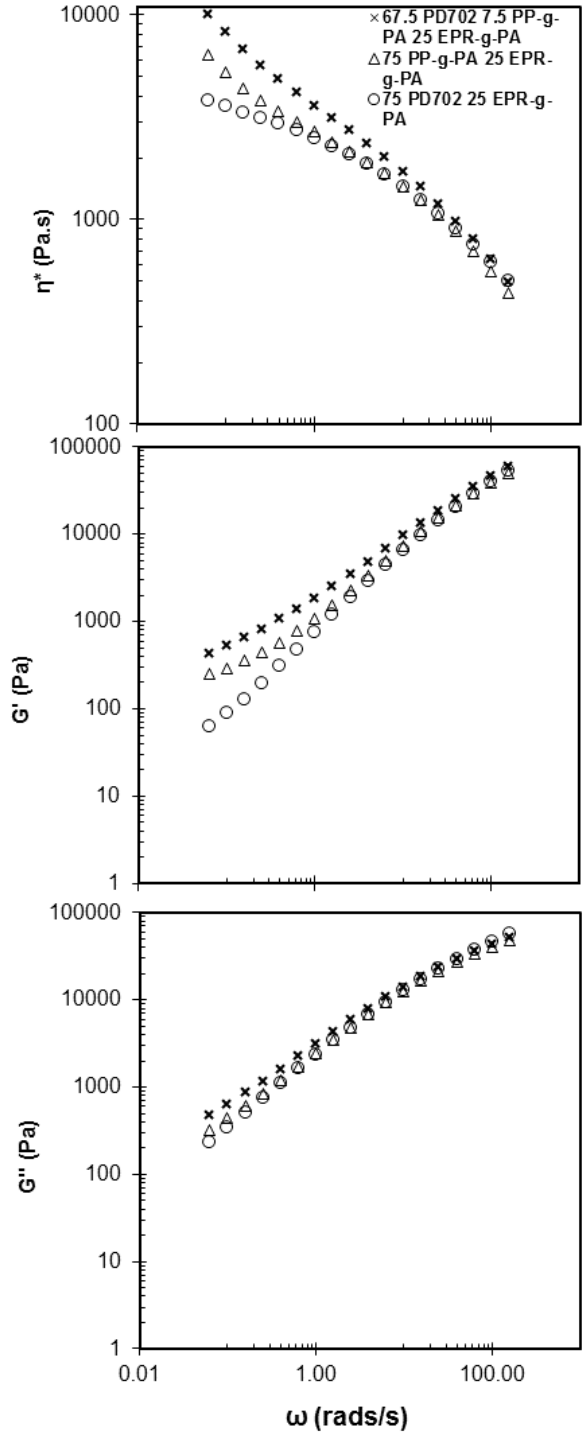

Figure 4.10. Effect of PP-g-PA on a) Complex viscosity, b) Storage modulus and c) Loss modulus, as a function of frequency for 25/75 EPR/PP blends at 180^{o}C.

Despite the similarity in the PP-g-PA and PD702 viscoelastic properties, shown in Figure 4.5, the EPR-g-PA/PP-g-PA displays substantially different rheological behavior than the EPR-g-PA/PD702 blend. Though there were negligible differences between the loss moduli (G'') the PA blend was found to have a greater complex viscosity and storage modulus at low frequencies. The low frequency plateau in G' observed in the PA blend and discussed in the last section was not evident in the PD702/EPR-g-PA blend. This supports that the low frequency deviation is related to the presence of the zwitterionic groups in the PP phase however it remains unclear whether the rheology is related to an interfacial effect or through the long range association of the EPR-g-PA droplets across the zwitterionic matrix.

The addition of zwitterionic functionality to the PD702/EPR-g-PA blend resulted in an increase in complex viscosity and an increase storage modulus, by nearly an order of magnitude at 0.06 rads/s, with a relatively small effect on loss modulus. An increase in viscosity is consistent with the expected rheology of a compatibilized TPV. The localization of compatibilizer chains at the interface reduces interfacial tension and improves interfacial adhesion due to the strong interfacial interactions. This has been observed in compatibilized TPVs, in which a strongly interacting interfacial area reduces interlayer slip facilitating stress transfer between matrix and elastomer inclusions, increasing viscosity.[84]

The rheology of the compatibilized blend is similar to what was observed in the PP-g-PA/EPR-g-PA blend. There is an inflection point in the storage modulus curve within the PD702 terminal zone, at approximately 2 rads/s, and the presence of a low frequency plateau which was not observed in the PD702/EPR-g-PA blend. Considering the low amount of PP-g-PA in the blend it is unlikely that the zwitterionic PP is spanning the distance between and bridging the EPR-g-PA droplets, suggesting that the low frequency elastic response observed in the PP/PP-g-PA/EPR-g-PA blend originates from the presence of the zwitterionic PP at the blend interface.

As discussed previously this effect has been reported in TPVs and composites, however similar behavior has also been observed in immiscible blends following addition of a compatibilizer. In physically compatibilized blends low frequency elasticity and deviation from the Palierne model have been

attributed to the shape relaxation of a compatibilizer phase encapsulating the dispersed phase.[16,83,85] This effect is believed to relate to Marangoni stresses, which are present due to a flow induced gradient in compatibilizer concentration across the inclusion surface during shearing.[16] While many compatibilized blends show an increase in elasticity at low frequencies, they typically fail to show the transition to solid-like behavior observed in the zwitterionomer compatibilized blends. This transition to solid-like behavior has however been reported in a number of reactively compatibilized blends, in which compatibilizers chains are grafted onto the dispersed phase surface, and has been observed in blends containing polyamides and maleic anhydride functional compatibilizers.[85-87] Rational for this effect remains somewhat controversial, citing either the presence a three-dimensional network through the interaction of grafted chains,[86,87] or the relaxation of a low mobility compatibilized zone surrounding the inclusions.[85] The fundamental cause or causes of this low frequency viscoelasticity in composites, TPVs and compatibilized blends, though described as two distinct effects, three-dimensional networks or shape relaxation, may have a common basis. The rheological results of the zwitterionic compatibilized blend in this work and the reactively compatibilized blends in literature are consistent with the rheology of composites and TPVs in which particle networks have been explicitly observed. The low frequency storage modulus plateau in some composites has been shown to strongly depend on the strength of its interfacial interactions with the matrix polymer. In silica composites the transition to solid-like behavior was believed to be related to the networking of polymer chains adsorbed to the filler silica.[79] This finding was supported by the decrease in low frequency modulus when silica particles were treated with organosilane to prevent polymer adsorption. Similar results have been reported by Zang et al. whom observed a low frequency plateau of the storage modulus in nanosilica/POE composites.[88] Surface modification of silica to reduce polymer adsorption prior to compounding was found to both eliminate this plateau and generate terminal rheological behavior in the nanocomposite.

In these zwitterionomer compatibilized blends the origin of the low frequency increased elasticity remains unclear, likely originating either from the shape relaxation of a low mobility elastic PP-g-PA phase

surrounding the EPR-g-PA droplets, through the presence of entanglements and zwitterionic interactions between PP-g-PA chains bound to adjacent EPR-g-PA droplets or some combination of these effects. Its similar rheology to reactively compatibilized blends suggests the formation of strong interactions, likely in the form of multiplets at the interface between PP-g-PA and EPR-g-PA, similar to the presence of covalently bound graft chains.

4.4.7 Conclusion

Immiscible blends of EPR-g-PA and PP-g-PA exhibited substantial improvements in droplet dispersion, tensile elongation and impact strength relative to their precursor blends of EPR-g-MAn and PP-g-MAn. These improvements were attributed to the interaction between the zwitterionic multiplets of their component phases, which were substantially stronger than the polar interactions between the maleic anhydride functionalities.

The presence of zwitterionic interactions at the PP-g-PA EPR-g-PA interface was further supported by the zwitterionic blends frequency dependent viscoelasticity which was found to deviate substantially from that of conventional immiscible blends, exhibiting behavior more consistent with reactively compatibilized blends.

Blends of EPR-g-PA and i-PP incorporating small amounts of PP-g-PA also exhibited similar viscoelastic behavior in addition to substantial improvements in both morphology and mechanical properties. These results suggest the preferential localization of PP-g-PA at the interface, improving compatibility between PP and EPR-g-PA.

4.5 Work Cited

[1] C. B. Bucknall, D. Clayton, W. Keast, *J.Mater.Sci.* **1972**, *7*, 1443-1453.

[2] R. J. M. Borggreve, R. J. Gaymans, J. Schuijer, *Polymer*. **1989**, *30*, 71-77.

[3] L. A. Utracki, C. A. Wilkie, *Polymer blends handbook*, Springer Reference 2014.

[4] A. F. Yee, R. A. Pearson, *J.Mater.Sci.* **1986**, *21*, 2462-2474.

[5] C. B. Bucknall, *Toughened plastics*, Springer 1977.

[6] R. A. Pearson, A. F. Yee, *J.Mater.Sci.* **1986**, *21*, 2475-2488.

[7] R. Borggreve, R. J. Gaymans, J. Schuijer, *Polymer.* **1989**, *30*, 71-77.

[8] Y. Yokoyama, T. Ricco, *Polymer.* **1998**, *39*, 3675-3681.

[9] L. A. Utracki, B. D. Favis, *Polymer alloys and blends*, Marcel Dekker: New York 1989.

[10] D. R. Paul, *Polymer blends*, Elsevier 2012.

[11] J. Barlow, D. R. Paul, *Polymer Engineering & Science.* **1984**, *24*, 525-534.

[12] N. C. Liu, W. E. Baker, *Adv.Polym.Technol.* **1992**, *11*, 249-262.

[13] C. W. Macosko, P. Guegan, A. K. Khandpur, A. Nakayama, P. Marechal, T. Inoue, *Macromolecules.* **1996**, *29*, 5590-5598.

[14] P. Smith, A. Eisenberg, *J.Polym.Sci.B Polym.Lett.Ed.* **1983**, *21*, 223-230.

[15] U. Sundararaj, C. W. Macosko, *Macromolecules.* **1995**, *28*, 2647-2657.

[16] S. Velankar, P. Van Puyvelde, J. Mewis, P. Moldenaers, *Journal of Rheology (1978-present).* **2001**, *45*, 1007-1019.

[17] S. Danesi, R. S. Porter, *Polymer.* **1978**, *19*, 448-457.

[18] D. J. Lohse, S. Datta, E. N. Kresge, *Macromolecules.* **1991**, *24*, 561-566.

[19] S. Datta, D. J. Lohse, *Macromolecules.* **1993**, *26*, 2064-2076.

[20] A. Eisenberg, *Macromolecules.* **1970**, *3*, 147-154.

[21] A. Eisenberg, B. Hird, R. B. Moore, *Macromolecules.* **1990**, *23*, 4098-4107.

[22] X. Lu, R. A. Weiss, *Macromolecules.* **1991**, *24*, 4381-4385.

[23] A. R. Bhattacharyya, A. K. Ghosh, A. Misra, *Polymer.* **2003**, *44*, 1725-1732.

[24] P. Leewajanakul, R. Pattanaolarn, J. W. Ellis, M. Nithitanakul, B. P. Grady, *J Appl Polym Sci.* **2003**, *89*, 620-629.

[25] Y. Kim, C. Ha, T. Kang, Y. Kim, W. Cho, *J Appl Polym Sci.* **1994**, *51*, 1453-1461.

[26] A. Powell, M. Kontopoulou, S. Hojabr, *Macromol.React.Eng.* **2014**, *8*, 112-121.

[27] N. G. Gaylord, M. K. Mishra, *J.Polym.Sci.B Polym.Lett.Ed.* **1983**, *21*, 23-30.

[28] B. De Roover, M. Sclavons, V. Carlier, J. Devaux, R. Legras, A. Momtaz, *J.Polym.Sci.A Polym.Chem.* **1995**, *33*, 829-842.

[29] J. X. Li, W. L. Cheung, D. M. Jia, *Polymer.* **1999**, *40*, 1219-1222.

[30] M. Sclavons, V. Carlier, B. De Roover, P. Franquinet, J. Devaux, R. Legras, *J Appl Polym Sci.* **1996**, *62*, 1205-1210.

[31] Y. Wang, D. Ji, C. Yang, H. Zhang, C. Qin, B. Huang, *J Appl Polym Sci.* **1994**, *52*, 1411-1417.

[32] J. A. Lee, M. Kontopoulou, J. S. Parent, *Polymer.* **2005**, *46*, 5040-5049.

[33] Y. Loo, K. Wakabayashi, Y. E. Huang, R. A. Register, B. S. Hsiao, *Polymer.* **2005**, *46*, 5118-5124.

[34] S. I. Yoo, T. Y. Lee, J. Yoon, I. Lee, M. Kim, H. S. Lee, *J Appl Polym Sci.* **2002**, *83*, 767-776.

[35] C. L. Marx, S. L. Cooper, *Journal of Macromolecular Science, Part B.* **1974**, *9*, 19-33.

[36] E. B. Orler, D. J. Yontz, R. B. Moore, *Macromolecules.* **1993**, *26*, 5157-5160.

[37] Y. S. Yadav, P. C. Jain, *Polymer.* **1986**, *27*, 721-727.

[38] R. Paukkeri, A. Lehtinen, *Polymer.* **1993**, *34*, 4083-4088.

[39] E. Hirasawa, Y. Yamamoto, K. Tadano, S. Yano, *Macromolecules.* **1989**, *22*, 2776-2780.

[40] E. B. Orler, R. B. Moore, *Macromolecules.* **1994**, *27*, 4774-4780.

[41] N. K. Tierney, R. A. Register, *Macromolecules.* **2002**, *35*, 2358-2364.

[42] J. Yu, J. He, *Polymer.* **2000**, *41*, 891-898.

[43] K. Ishida, S. Han, Y. Inoue, S. Im, *Macromol.Chem.Phys.* **2005**, *206*, 1028-1034.

[44] K. Wakabayashi, R. A. Register, *Macromolecules.* **2006**, *39*, 1079-1086.

[45] S. Robert, *Morphological origins of the nonlinear mechanical properties of semicrystalline ionomers***, 2009**.

[46] K. Tadano, E. Hirasawa, H. Yamamoto, S. Yano, *Macromolecules.* **1989**, *22*, 226-233.

[47] M. Zhang, X. Yuan, L. Wang, T. C. M. Chung, T. Huang, W. deGroot, *Macromolecules.* **2014**, *47*, 571-581.

[48] R. A. Weiss, P. K. Agarwal, *J Appl Polym Sci.* **1981**, *26*, 449-462.

[49] L. M. Landoll, D. S. Breslow, *J.Polym.Sci.A Polym.Chem.* **1989**, *27*, 2189-2201.

[50] R. M. Ho, A. C. Su, C. H. Wu, S. I. Chen, *Polymer.* **1993**, *34*, 3264-3269.

[51] B. D. Favis, J. P. Chalifoux, *Polym.Eng.Sci.* **1987**, *27*, 1591-1600.

[52] H. Veenstra, J. Van Dam, d. B. Posthuma, *Polymer.* **2000**, *41*, 3037-3045.

[53] Z. Yuan, B. D. Favis, *AICHE J.* **2005**, *51*, 271-280.

[54] Z. Yuan, B. D. Favis, *Biomaterials.* **2004**, *25*, 2161-2170.

[55] J. A. Galloway, H. K. Jeon, J. R. Bell, C. W. Macosko, *Polymer.* **2005**, *46*, 183-191.

[56] H. Veenstra, J. Van Dam, d. B. Posthuma, *Polymer.* **1999**, *40*, 1119-1130.

[57] A. GonzÃ¡lez-Montiel, H. Keskkula, D. R. Paul, *J.Polym.Sci.B Polym.Phys.* **1995**, *33*, 1751-1767.

[58] W. S. Chow, Z. A. Mohd Ishak, J. Karger-Kocsis, A. A. Apostolov, U. S. Ishiaku, *Polymer.* **2003**, *44*, 7427-7440.

[59] T. A. Vilgis, J. Noolandi, *Macromolecules.* **1990**, *23*, 2941-2947.

[60] N. Dan, M. Tirrell, *Macromolecules.* **1993**, *26*, 637-642.

[61] J. M. Willis, B. D. Favis, *Polym.Eng.Sci.* **1988**, *28*, 1416-1426.

[62] J. M. Willis, V. Caldas, B. D. Favis, *J.Mater.Sci.* **1991**, *26*, 4742-4750.

[63] S. Wu, *Polymer.* **1985**, *26*, 1855-1863.

[64] R. Borggreve, R. J. Gaymans, H. M. Eichenwald, *Polymer.* **1989**, *30*, 78-83.

[65] C. B. Bucknall, V. L. P. Soares, H. H. Yang, X. C. Zhang, *Macromol.Symp.* **1996**, *101*, 265-271.

[66] d. W. van, R. Nijhof, R. J. Gaymans, *Polymer.* **1999**, *40*, 6031-6044.

[67] d. W. Van, A. Verheul, R. J. Gaymans, *Polymer.* **1999**, *40*, 6057-6065.

[68] B. Kuriakose, S. K. Chakraborty, S. K. De, *Mater.Chem.Phys.* **1985**, *12*, 157-170.

[69] T. Nomura, T. Nishio, T. Fujii, J. Sakai, M. Yamamoto, A. Uemura, M. Kakugo, *Polym.Eng.Sci.* **1995**, *35*, 1261-1271.

[70] D. Graebling, R. Muller, *Journal of Rheology.* **1990**, *34*, 193-205.

[71] B. Brahimi, A. Ait-Kadi, A. Ajji, R. Jérôme, R. Fayt, *Journal of Rheology.* **1991**, *35*, 1069-1091.

[72] C. Tucker III L., P. Moldenaers, *Annu.Rev.Fluid Mech.* **2002**, *34*, 177-210.

[73] J. F. Palierne, *Rheologica Acta.* **1990**, *29*, 204-214.

[74] D. Graebling, R. Muller, J. F. Palierne, *Macromolecules.* **1993**, *26*, 320-329.

[75] D. Graebling, A. Benkira, Y. Gallot, R. Muller, *European Polymer Journal.* **1994**, *30*, 301-308.

[76] C. Lacroix, M. Bousmina, P. J. Carreau, B. D. Favis, A. Michel, *Polymer.* **1996**, *37*, 2939-2947.

[77] M. Bousmina, R. Muller, *Journal of Rheology.* **1993**, *37*, 663-679.

[78] M. Hemmati, H. Nazokdast, H. Shariat Panahi, *J Appl Polym Sci.* **2001**, *82*, 1129-1137.

[79] M. I. Aranguren, E. Mora, J. V. DeGroot, C. W. Macosko, *Journal of Rheology (1978-present).* **1992**, *36*, 1165-1182.

[80] W. G. F. Sengers, P. Sengupta, J. W. M. Noordermeer, S. J. Picken, A. D. Gotsis, *Polymer.* **2004**, *45*, 8881-8891.

[81] P. Bardollet, M. Bousmina, R. Muller, *Polym.Adv.Technol.* **1995**, *6*, 301-308.

[82] M. Bousmina, R. Muller, *Rheologica Acta.* **1996**, *35*, 369-381.

[83] R. -. Riemann, H. -. Cantow, C. Friedrich, *Macromolecules.* **1997**, *30*, 5476-5484.

[84] S. George, K. Ramamurthy, J. S. Anand, G. Groeninckx, K. T. Varughese, S. Thomas, *Polymer.* **1999**, *40*, 4325-4344.

[85] M. Moan, J. Huitric, P. Médéric, J. Jarrin, *Journal of Rheology.* **2000**, *44*, 1227-1245.

[86] C. Sailer, U. A. Handge, *Macromolecules.* **2007**, *40*, 2019-2028.

[87] C. Sailer, U. A. Handge, *Macromolecules.* **2008**, *41*, 4258-4267.

[88] Q. Zhang, L. A. Archer, *Langmuir.* **2002**, *18*, 10435-10442.

Chapter 5

Conclusions and Recommendations

5.1 Conclusions

Zwitterionic derivatives of an ethylene-propylene copolymer (EPR-g-PA) and polypropylene (PP-g-PA) were synthesized through a reaction of their maleated precursors with a tertiary amino alcohol, yielding grafted ammonium and carboxylate functional groups.

Following its conversion EPR-g-PA exhibited a large increase in viscoelasticity, evident in both its oscillatory and extensional behavior, and an increase in tensile strength, with properties similar to a lightly cross-linked EPR. Relative to EPR-g-MAn, EPR-g-PA also exhibited considerable changes in its adhesive properties, substantially increasing its adhesion to ionomer substrates. The presence and interaction of zwitterionic multiplets in EPR-g-PA were believed to be responsible for these behaviors, forming physical crosslinks due to attractive electrostatic forces between the ionic moieties.

Conversion of PP-g-MAn to PP-g-PA had a marginal effect on its properties, exhibiting an increase in crystallization onset temperature but a negligible effect on total crystallinity, viscoelasticity and mechanical properties. These results were believed to result from its relatively low ionic content, which may be insufficient to substantially alter its behavior, and may also suggest that the zwitterionic groups primarily exist as isolated ion pairs or small multiplets rather than forming larger ionic aggregates.

Blends prepared by the in-situ reaction of EPR-g-MAn with DMAEE during compounding with PP produced a blend with superior impact properties compared to a similar blend of EPR and PP in which the elastomer phase was cross-linked in-situ using a peroxide. This difference was attributed to the radical induced degradation of the PP phase which is a consequence of peroxide mediated cross-linking in thermoplastic vulcanizate blends incorporating PP. Physical crosslinking of the elastomer phase by the introduction of zwitterionic functionality offers a viable alternative to produce lightly cross-linked TPVs

with improved strength, without suffering from the side effects of lower ductility and loss of PP strength typical of peroxide-cured systems.

The addition small amounts of PP-g-PA to immiscible blends of EPR-g-PA and PP substantially improved droplet dispersion, tensile elongation and impact strength. These improvements were attributed to decreased interfacial tension, reduced droplet coalescence and improved interfacial adhesion resulting from the interaction of zwitterionic functionality of PP-g-PA and EPR-g-PA at the phase interface. The viscoelastic properties of these zwitterionic blends were atypical of conventional immiscible blends exhibiting behavior that deviated from Palierne emulsion model predictions at low frequencies. This behavior was however similar to the viscoelastic behavior of reactively compatibilized blends further suggesting the presence of strong associations at the phase interface.

5.2 Recommendations for future work

5.2.1 High maleic anhydride graft content

The properties of ionomers are heavily dependent on their ionic concentration, frequently exhibiting dramatic changes in viscoelasticity and mechanical properties beyond a critical ionic concentration, usually cited around 2-6mol%.[1-3] These changes are believed to relate to changes in ionomer microstructure from isolated multiplets to ionic clusters capable of acting as reinforcing filler. The ionic content of the zwitterionomers synthesized from maleated polymers and DMAEE is limited by the amount of graft succinic anhydride. Despite the importance of ion clusters in conventional ionomers there has been little work examining the presence of zwitterionic clusters and their effect on zwitterionomer properties. This work examined polymers with relatively low graft content, less than 0.5 mol%, substantially below the expected critical ionic concentration. Using a maleated polymer with high graft content, ~6mol%, will facilitate the study of the degree of neutralization on this zwitterionomer's properties. The presence of clusters may be detected by small angle X-ray scattering, [4] and their effect on properties may be examined by rheology and mechanical testing.

5.2.2 Comparison with metal neutralized ionomers

While PP-g-PA and EPR-g-PA exhibited interesting changes in properties it remains unclear what advantages these materials might have over classic metal neutralized ionomers. More conventional ionomers can be synthesized by hydrolyzing the succinic anhydride groups of PP-g-MAn and EPR-g-MAn and neutralizing them with a metal cation.[5,6] This could provide a direct comparison between zwitterionic ionomers and metal-neutralized ionomers and can assist in clarifying the potential value of this new class of zwitterionic materials.

5.2.3 Anti-fouling properties

In recent years there has been substantial interest in the use of zwitterionic materials for surface modification due to their anti-fouling properties. A wide range of zwitterionic structures have shown a high resistance to the adsorption of proteins, an effect which is believed to relate to their inter-zwitterionic associations.[7,8] The unique zwitterionic functionality present in PP-g-PA and EPR-g-PA were shown capable of forming physical crosslinks due strong Coulombic interactions between their functional groups, which may suggest its similar capacity to resist fouling. This property might be effectively studied using optical, spectroscopic or solution depletion techniques.[9]

5.3 Work Cited

[1] A. Eisenberg, M. Navratil, *Macromolecules.* **1974***, 7*, 90-94.

[2] D. G. Peiffer, R. A. Weiss, R. D. Lundberg, *Journal of Polymer Science: Polymer Physics Edition.* **1982***, 20*, 1503-1509.

[3] J. J. Fitzgerald, R. A. Weiss, *Journal of Macromolecular Science, Part C.* **1988***, 28*, 99-185.

[4] D. J. Yarusso, S. L. Cooper, *Polymer.* **1985***, 26*, 371-378.

[5] J. Yu, J. He, *Polymer.* **2000***, 41*, 891-898.

[6] B. P. Grady, J. G. P. Goossens, M. E. L. Wouters, *Macromolecules.* **2004***, 37*, 8585-8591.

[7] P. Lin, C. Lin, R. Mansour, F. Gu, *Biosensors and Bioelectronics.* **2013***, 47*, 451-460.

[8] J. B. Schlenoff, *Langmuir.* **2014***, 30*, 9625-9636.

[9] V. Hlady, J. Buijs, H. P. Jennissen, *Meth.Enzymol.* **1999***, 309*, 402-429.